doi : 10.17596/0003294

KAIREI Cruise Report

KR10-12

Studies on the thermal structure and the water distribution in the upper part of the Pacific plate subducting along the Japan Trench

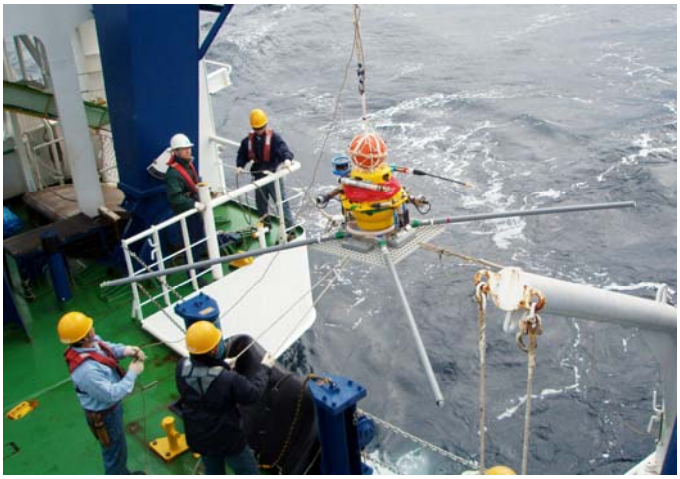

Japan Trench area

November 14, 2010 – November 29, 2010

Japan Agency for Marine-Earth Science and Technology

(JAMSTEC)

Contents

1. Cruise Information

Cruise number:

KR10-12

Ship name:

R/V KAIREI

Title of the cruise:

2010 Deep Sea Research
Research cruise with KAIREI

Title of proposal:

S10-59
Studies on the thermal structure and the water distribution in the upper part of the Pacific plate subducting along the Japan Trench

Cruise period:

November 14, 2010 – November 29, 2010

Port call:

2010 Nov. 14 Dept. from Yokosuka (JAMSTEC)
Nov. 29 Arriv. at Yokosuka (JAMSTEC)

Research area:

Japan Trench area and a station off the Boso Peninsula

Research map:

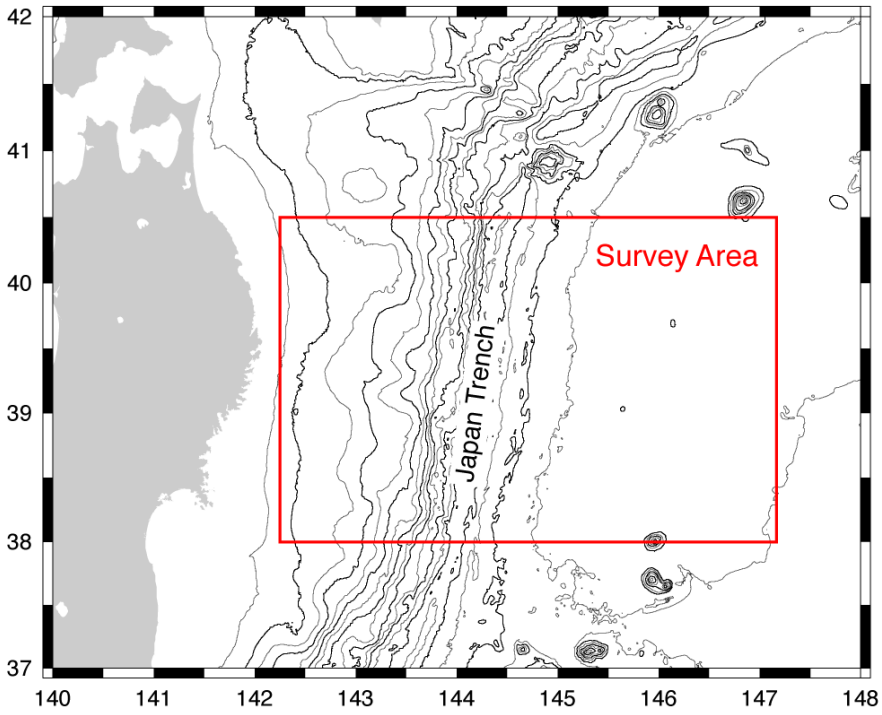

Figure 1-1. Survey area around the Japan Trench

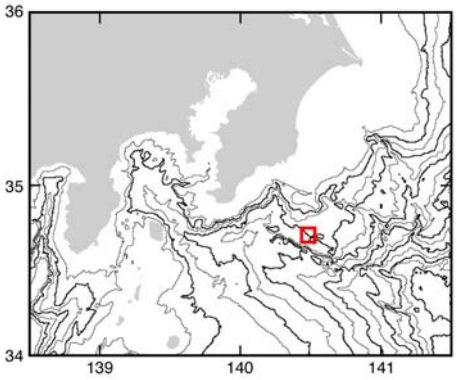

Figure 1-2. Station off the Boso Peninsula

Ship track and observation points are shown in 3.2.3.

2. Researchers

Chief Scientist:

Makoto YAMANO	Earthquake Research Institute, University of Tokyo	

Science Party:

Makoto YAMANO	Earthquake Research Institute, University of Tokyo	
Akiko TANAKA	Institute of Geology and Geoinformation, National Institute of Advanced Industrial Science and Technology	
Shusaku GOTO	Institute for Geo-Resources and Environment, National Institute of Advanced Industrial Science and Technology	
Kiichiro KAWAMURA	Fukada Geological Institute	
Takafumi KASAYA	IFREE, JAMSTEC	
Hiroshi ICHIHARA	IFREE, JAMSTEC	
Kiyoshi BABA	Earthquake Research Institute, University of Tokyo	
Chikaaki FUJITA	Earthquake Research Institute, University of Tokyo	
Madoka KOBAYASHI	Graduate School of Science, Hokkaido University	
Masataka KINOSHITA	IFREE, JAMSTEC	(shore-based)
Tada-nori GOTO	Graduate School of Engineering, Kyoto University	(shore-based)
Toshiya FUJIWARA	IFREE, JAMSTEC	(shore-based)
Yoshifumi KAWADA	IFREE, JAMSTEC	(shore-based)
Junji YAMAMOTO	Institute for Geothermal Sciences, Kyoto University	(shore-based)

Technical Support Staff

Kaoru TSUKUDA	Nippon Marine Enterprises, Ltd.
Yusuke SATO	Marine Works Japan, Ltd.
Yutaka MATSUURA	Marine Works Japan, Ltd.
Akira SO	Marine Works Japan, Ltd.
Kazuhiro YOSHIDA	Marine Works Japan, Ltd.

3. Observation

3.1. Introduction

In the Japan Trench subduction zone, an old oceanic plate with an age of over 100 m.y., the Pacific plate, is subducting beneath the northeast Japan arc. Recent studies have revealed that the Pacific plate just before subduction may not be uniformly cold contrary to its old age.

Yamano et al. (2008) conducted heat flow measurements on the seaward slope and the outer rise of the Japan Trench along a parallel of 38°45'N and showed the existence of high heat flow anomalies (Fig. 3.1.1). High heat flow values (70 to 115 mW/m^2) were obtained at many stations, while values normal for the seafloor age (about 50 mW/m^2) were also observed at some stations. It suggests that thermal structure of the Pacific plate in this area is not a typical one for old oceanic lithosphere, at least at shallow depths.

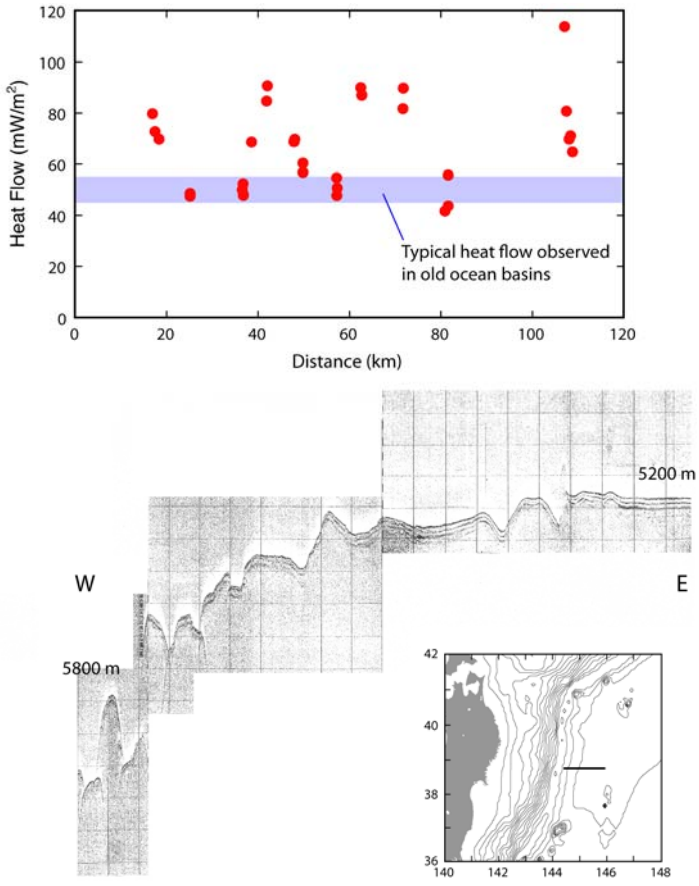

Figure 3.1-1. Heat flow profile on the seaward slope of the Japan Trench along a parallel of 38°45'N projected on a 3.5 kHz subbottom profiler record (Yamano et al., 2008).

Another recent finding is a peculiar type of intra-plate volcanism around the outer rise of the Japan Trench, called “petit-spot” (Hirano et al., 2001; 2006). Basaltic rocks with radiometric ages ranging from 4.2 to 8.5 m.y. were collected on the seaward slope of the trench and even younger rocks (younger than 1 m.y.) were found on the eastern edge of the outer rise. This

volcanism might provide a heat source of the observed high heat flow anomalies and exert a significant influence on the thermal structure of the Pacific plate.

Subduction of oceanic plate causes large thrust earthquakes along the interface with the overlying landward plate. The extent of the seismogenic zone of these earthquakes is thought to be controlled mainly by the temperature distribution along the plate interface (e.g., Oleskevich et al., 1999). The existence of water along the plate interface should also play important roles in the stress accumulation and rupture processes in the seismogenic zone. In the Japan Trench subduction zone, the nature of the seismogenic zone, such as seismicity, size of asperities and coupling of the plates, significantly varies along the trench (e.g., Yamanaka and Kikuchi, 2004). Such variations could be related to the temperature structure and water content along the plate interface.

It is therefore important to accurately estimate the temperature structure around the plate interface for studies of seismogenic processes in the Japan Trench subduction zone. We, however, do not have surface heat flow data enough to constrain the thermal model of the subduction zone. It is necessary to conduct more systematic and dense heat flow measurements both on the seaward and landward slopes of the trench.

Results of electromagnetic survey conducted on the landward slope of the Japan Trench show that the subducted oceanic crust has high electrical conductivity and thus contains a large amount of water (Goto et al., 2001), though we do not know where and how the water penetrated into the crust. It is critically important to clarify the penetration process and distribution of the water in the oceanic crust for investigation of the mechanical properties of the plate interface.

In consideration of importance of knowing the temperature and electrical conductivity structures of the subducting Pacific plate, we started a research project “Studies on the thermal structure and the water distribution in the upper part of the Pacific plate subducting along the Japan Trench” in 2007, supported by a Grant-in Aid for Scientific Research (19340125) from JSPS. Within the framework of this project, we conducted heat flow measurements and electromagnetic surveys in the Japan Trench area on five cruises (KH-07-3 of R/V Hakuho-maru, KR08-10 and KR09-16 of R/V Kairei with ROV Kaiko 7000II, KT-08-25 and KT-09-8 of R/V Tansei-maru). The research plan of this cruise (KR10-12) was made based on the results of the previous five cruises as shown in the following sections and the data we obtained on this cruise will be analyzed and/or synthesized with them.

3.2. Summary of the Cruise

3.2.1. Research items

(1) Heat flow measurement

Measurement of temperature profiles in surface sediment with ordinary deep-sea heat flow probes for determination of terrestrial heat flow.

(2) Long-term temperature monitoring on the seafloor

Long-term monitoring of the bottom water temperature using a pop-up type instrument for evaluation of influence of water temperature variation on heat flow measurement.

(3) Sediment core sampling with heat flow measurement (HFPC)

Sampling of surface sediments with a piston corer and heat flow measurement at the same site using temperature sensors mounted on the core barrel.

(4) Ocean-bottom electromagnetic survey

Mesurement of electromagnetic fields on the seafloor with high-frequency ocean-bottom electromagnetometers (HF-OBEMs) and long-term ocean-bottom electromagnetometers (LT-OBEMs) for magnetotelluric survey.

(5) Bathymetry and geophysical survey

Bathymetry mapping with a multi narrow beam system, gravity measurement, and measurements of total magnetic field and geomagnetic vector.

3.2.2. Cruise schedule and operations

Date	Events, Operations
Nov. 14	Leave Yokosuka (JAMSTEC) Arrive at the station off the Boso Peninsula Recovery of a pop-up water temperature monitoring system (PWT1) Transit to the survey area
Nov. 15	Arrive in the survey area Deployment of three HF-OBEMs (C11, B11 and B12) Bathymetry survey
Nov. 16	Deployment of two LT-OBEMs (B13 and B14) Bathymetry and geophysical survey
Nov. 17	Piston core sampling with heat flow measurement (HFPC01) Heat flow measurement (HF01) Transit to Miyako Inlet
Nov. 18	Disembarkation of scientists (Miyako) Take refuge from rough sea (Miyako Inlet) Transit to the survey area
Nov. 19	Heat flow measurement (HF02) Bathymetry and geophysical survey
Nov. 20	Piston core sampling with heat flow measurement (HFPC02) Heat flow measurement (HF03) Bathymetry and geophysical survey
Nov. 21	Heat flow measurement (HF04) Heat flow measurement (HF05) Bathymetry and geophysical survey
Nov. 22	Heat flow measurement (HF06) Heat flow measurement (HF07) Bathymetry and geophysical survey
Nov. 23	Take refuge from rough sea (off Ishinomaki)
Nov. 24	Take refuge from rough sea (off Ishinomaki) Transit to the survey area
Nov. 25	Wait for the sea condition to recover in the survey area
Nov. 26	Recovery of three HF-OBEMs (C11, B11 and B12) Bathymetry and geophysical survey
Nov. 27	Wait for the sea condition to recover in the survey area

	Piston core sampling with heat flow measurement (HFPC03) Leave the survey area
Nov. 28	Transit to Yokosuka Arrive in Tokyo Bay
Nov. 29	Arrive at Yokosuka (JAMSTEC)

Detailed cruise log is given in the Appendices (7-1).

3.2.3. Ship track and observation points

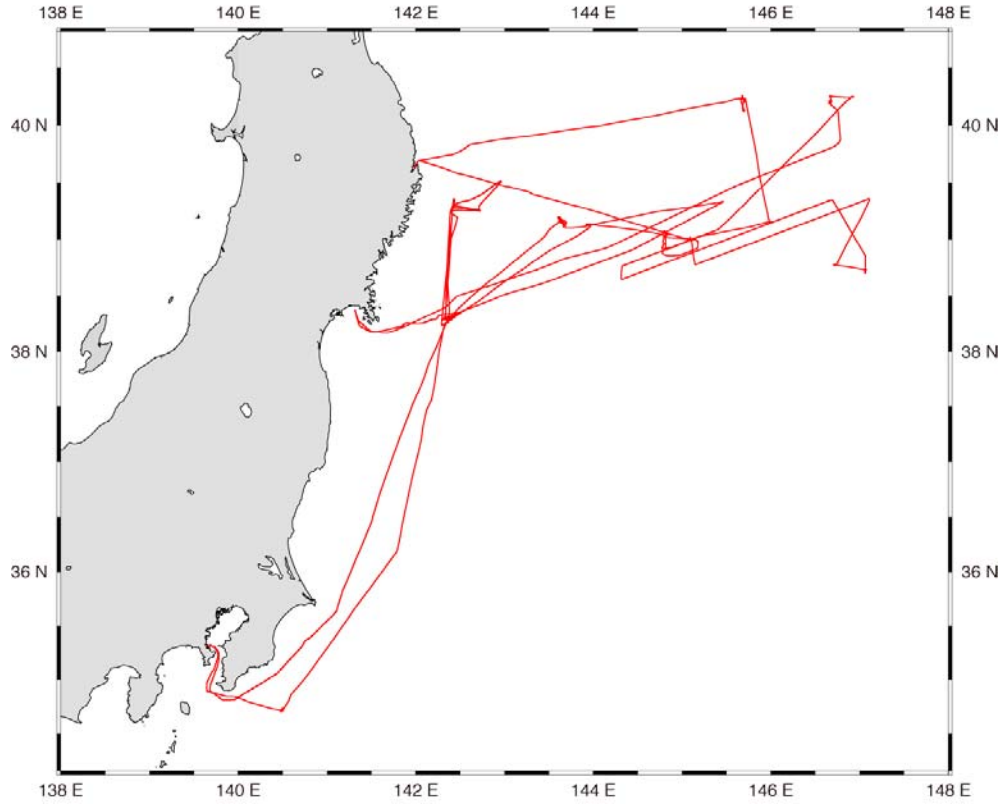

Figure 3.2-1. Ship track of KR10-12 cruise.

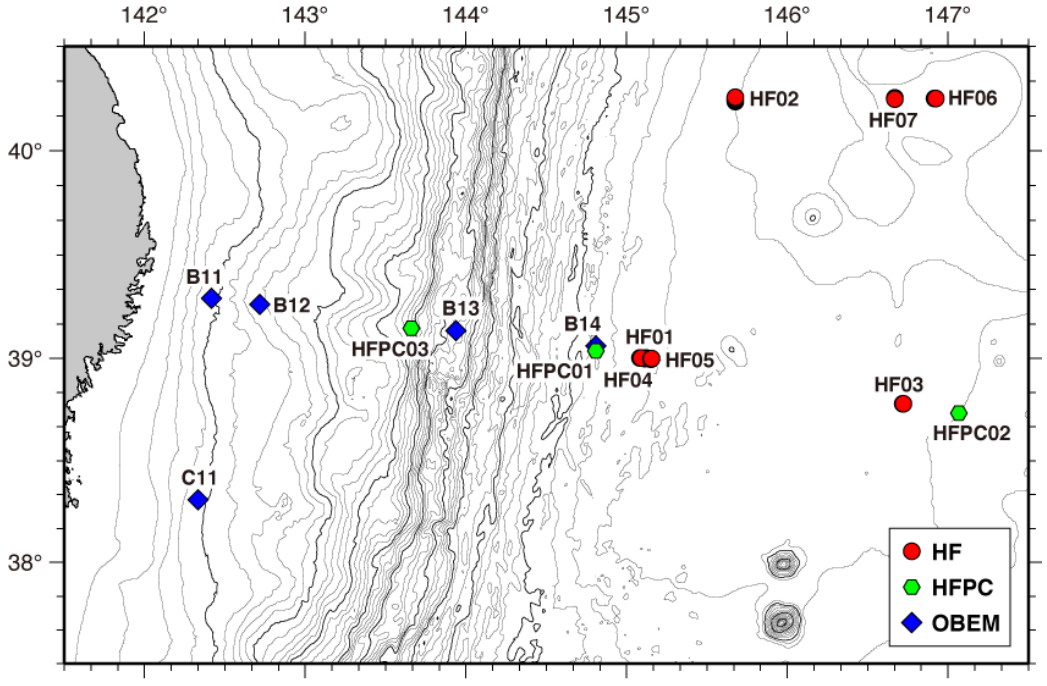

Figure 3.2-2. Measurement and sampling stations in the Japan Trench area.

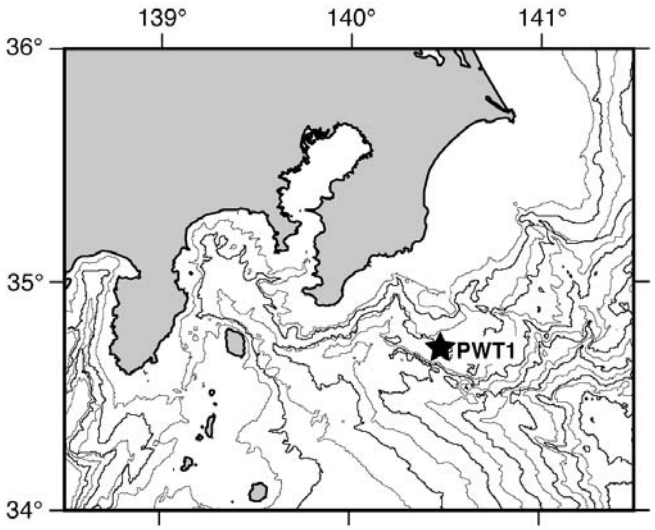

Figure 3.2-3. Measurement station off the Boso Peninsula.

3.3. Research Objectives

We intend to clarify the temperature structure and the water distribution in the upper part of the Pacific plate subducting beneath the northeast Japan arc through heat flow measurements and electromagnetic surveys in the Japan Trench area. Based on the obtained results, we will investigate intra-plate volcanism on the Pacific plate, heat transfer and water movement in the oceanic crust associated with development of normal faults on the seaward slope of the Japan Trench. We also intend to examine relation between the temperature structure and water distribution along the subducting plate boundary and mechanical properties of the seismogenic zone.

3.3.1. Heat flow measurement

Heat flow values measured on the seaward slope of the Japan Trench along a parallel of 38°45'N are high at some locations and normal for the seafloor age at others (Yamano et al., 2008; Fig. 3.1-1). A possible cause of the spatial variation of heat flow is fluid flow along normal faults developed on the seaward slope of the trench, although no clear correlation between the heat flow distribution and the seafloor topography is recognized. The high average heat flow requires the existence of some heat source in the upper part of the plate. The heat source may be provided by intra-plate ("petit-spot") volcanism taking place around the outer rise.

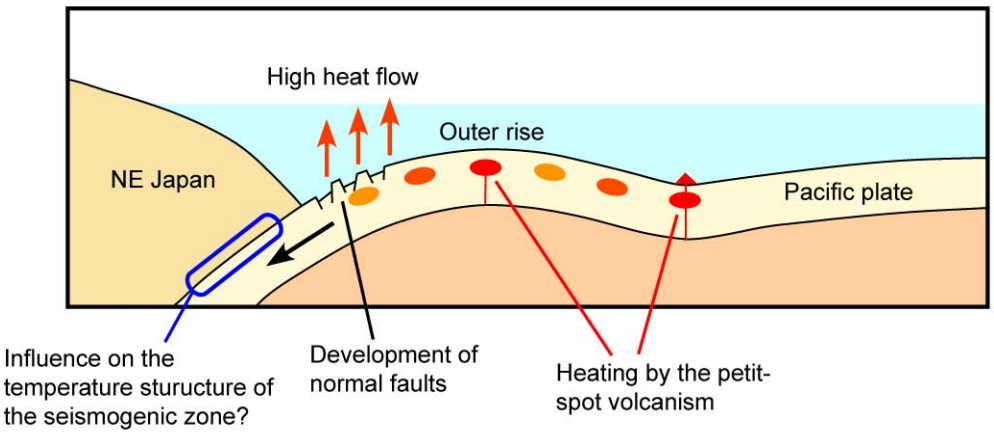

Figure 3.3-1. Schematic model of possible processes giving high heat flow on the seaward slope of the Japan Trench (Yamano et al., 2008).

A qualitative model which may account for the observed heat flow is shown in Fig. 3.3-1. When the Pacific plate reaches the trench outer rise area, melts produced by the petit-spot volcanism repeatedly intrude into the uppermost mantle and/or the lower crust with some eruption at the seafloor, and heat the surroundings. Then development of normal faults in the vicinity of the trench allows fluid flow along the fault zones, which carry heat and focus heat

loss from the layers heated by intrusions. The effective vertical thermal diffusivity may vary from place to place depending on the permeability of fault zones and result in variable heat flow.

The model presented above is rather speculative and needs to be improved through more geophysical and petrological studies, including detailed heat flow surveys. It is necessary to conduct measurements at different latitudes, to make dense measurements around sites with high values, and to investigate relationship between the heat flow distribution and the crustal structure.

The thermal structure of the subducting plate is one of the key factors which control the temperature distribution of the plate interface including the seismogenic zone of large thrust earthquakes. Subduction of the plate, the upper part of which has been anomalously heated, would result in an anomalous temperature structure along the plate interface, affecting mechanical properties of the seismogenic zone.

We chose three lines across the northern Japan Trench (lines A, B, and C in Fig. 3.3-2), along which seismic refraction and reflection surveys were conducted (Tsuru et al., 2000: Ito et al., 2004: Miura et al., 2005), as survey lines for the research project “Studies on the thermal structure and the water distribution in the upper part of the Pacific plate subducting along the Japan Trench” (cf. 3.1). The three lines go through regions with different degrees of seismic coupling along the subduction plate interface (e.g., Yamanaka and Kikuchi, 2004). Comparison of temperature and electrical conductivity structures along these lines will provide information on physical processes in the seismogenic zone.

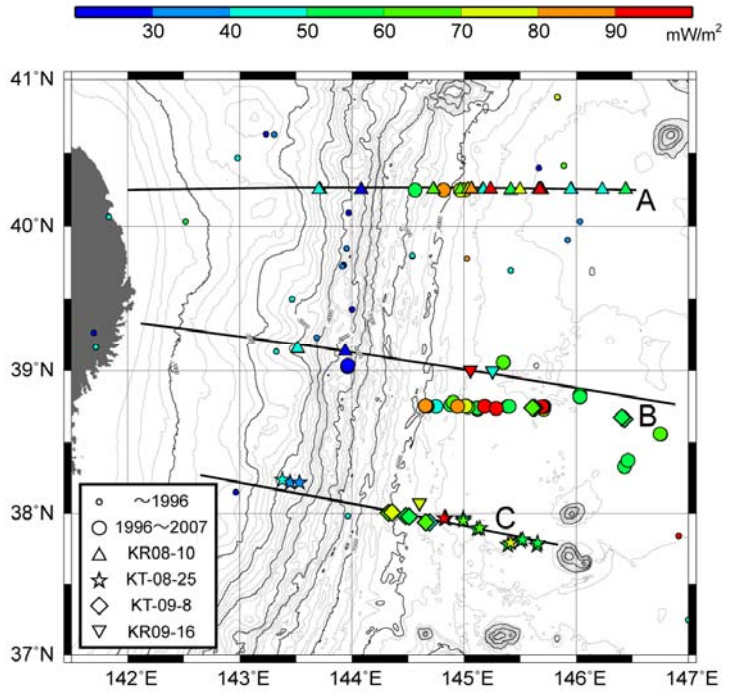

Figure 3.3-2. Heat flow data in the northern Japan Trench area.

Along a parallel of 38°45'N on the seaward side of the Japan Trench, close to the seaward part of the line B, relatively dense heat flow surveys had been made by Yamano et al. (2008). In the project, therefore, we have conducted heat flow measurements mainly along the lines A and C, and the landward part of the line B (Fig. 3.3-2). New data obtained on the previous five cruises (KH-07-3, KR08-10, KT-08-2, KT-09-8 and KR10-12) revealed that heat flow distributions on the seaward slope and outer rise of the trench along the lines A and C is similar to that along 38°45'N (Yamano et al., 2010). High values (higher than 70 mW/m^2) were measured at many stations, while normal values (about 50 mW/m^2) were obtained at other stations.

Main objectives on this cruise were: 1) to make measurements to the east of the existing data for delineation of the seaward extent of the high heat flow, and 2) to conduct dense measurements in the vicinities of stations with very high heat flow values in order to know the spatial scale of local anomalies. We also planned to conduct additional measurements on the landward slope of the trench to impose further constraint on the thermal structure of the subduction plate interface.

3.3.2. Natural source electromagnetic survey

Imaging of pore-fluid distribution is important theme for investigation of dynamics around subduction zones because it controls viscosity, shear strength and solidus temperature of rocks. Electromagnetic surveys are expected to constrain the fluid distribution because electrical conductivity is known as a good indicator for pore fluid in the crust and the uppermost mantle. However, few electromagnetic observations have been conducted in the marine area around NE Japan, although most of the NE Japan arc system is covered with seawater. In this cruise, we conducted marine MT surveys with OBEMs around the Japan Trench in order to elucidate following topics (Fig. 3.3-3). 1) How is the water included in the plate before subduction? 2) Seismic study showed low velocity zones in the interplate earthquake zone that may imply water distribution (Fujie et. al., 2002). Resistivity imaging by the OBEM survey will constrain the fluid distribution from different perspective. 3) Simulation implied large amount of aqueous water transportation and dehydration around the study area (Iwamori, 2007). OBEM survey also gives constraint for the dehydrated fluid.

We deployed and recovered eight OBEMs along the survey lines located near 40°N (line A), 39°N (line B), and 38°N (line C) in the previous cruises during 2008-2009 (Fig. 3.3-4). In this cruise, we deployed five OBEMs across the Japan Trench and recovered three of them (sites B11, B12, C11; type A OBEM) after about 11 days (Fig. 3.3-4). In order to obtain high S/N data in this short observation period, we planned to settle these OBEMs in relatively shallow water zones (950-1600 m deep). Two OBEMs (site B13, type A OBEM; site B14, type B OBEM) were planned to settle in deep water area (5400 m deep, 5800 m deep) on the landward

slope and will be recovered six months after. In order to obtain wide-band MT response at the site B13, we updated this OBEM that sampling rate can be changed at an arbitrary time during observations.

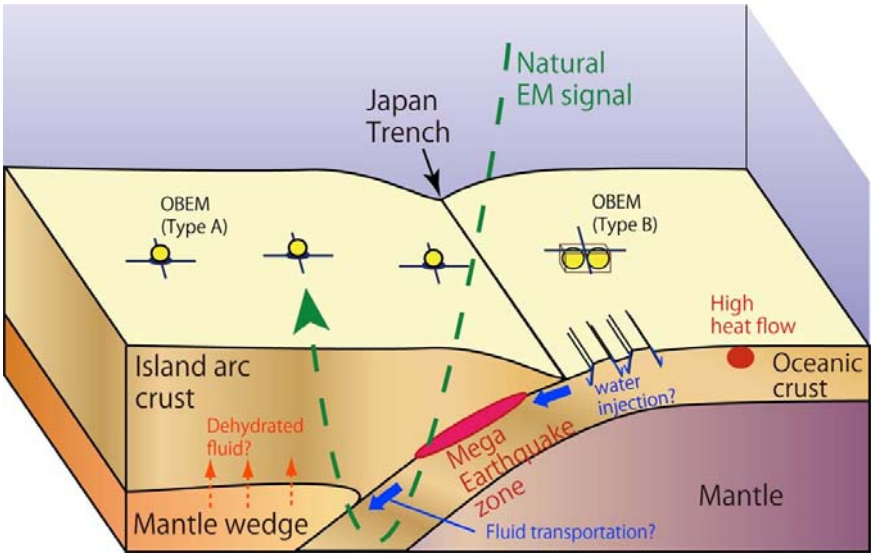

Figure 3.3-3. Schematic illustration of OBEM observation.

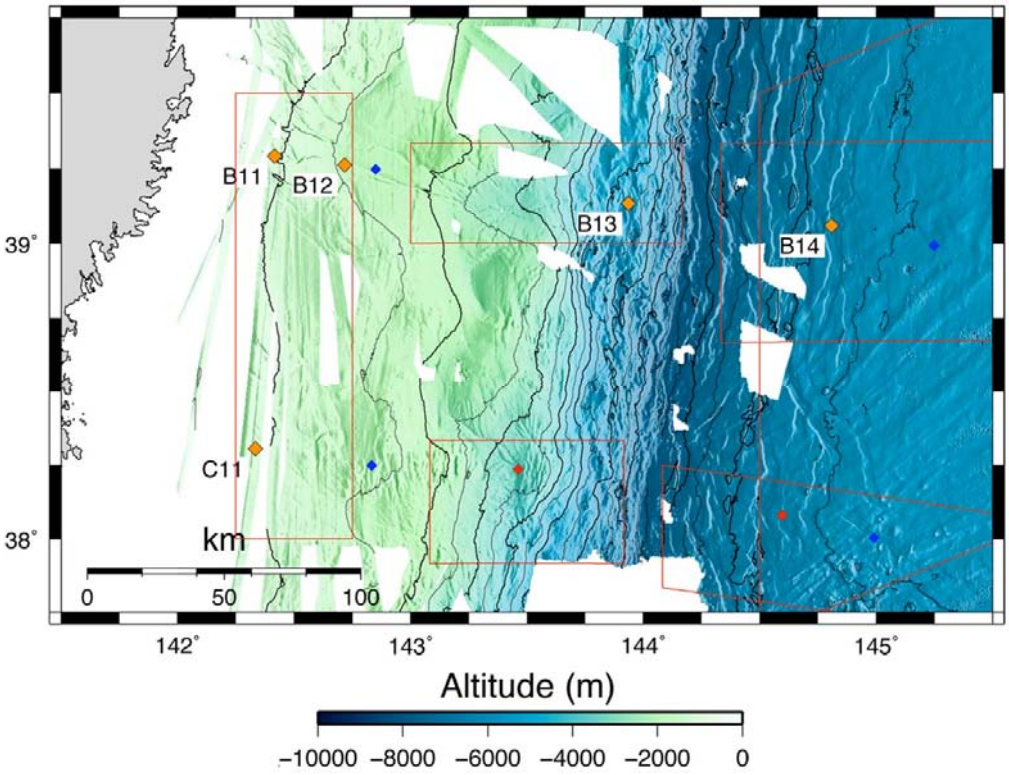

Figure 3.3-4. Index map of OBEM observation. Orange diamonds denotes OBEM sites settled in this cruse. Short and long term OBEM sites settled in the past cruises are also shown in red and blue diamonds, respectively.

3.4. Instruments and Operation Methods

3.4.1. Deep-sea heat flow probe

Heat flow is obtained as the product of the geothermal gradient and the thermal conductivity. We measured the geothermal gradient by penetrating an ordinary deep-sea heat flow probe or a heat flow piston corer (HFPC, cf. 3.4.2) into seafloor sediments.

[Specification of tools]

The deep-sea heat flow probe (Fig. 3.4-1) weighs about 800 kg and has a 3.0 m-long lance, along which seven compact temperature recorders (Miniaturized Temperature Data Logger, ANTARES Datensysteme GmbH; Fig. 3.4-2) are mounted in an outrigger fashion (Ewing type). A heat flow data logger (Kaiyo Denshi Co., DHF-650) placed inside the weight head (cf. Fig. 3.4-3) was used for recording the tilt and the depth of the probe. Tilt and depth data were sent to the surface with acoustic pulses so that we can monitor the status of the probe on the ship.

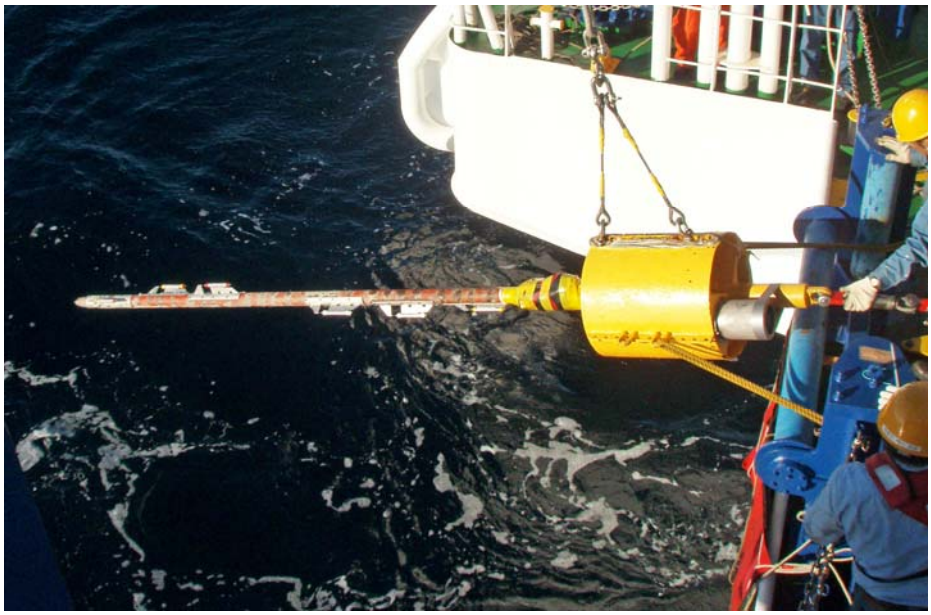

Figure 3.4-1. Deep-sea heat flow probe.

Figure 3.4-2. ANTARES Miniaturized Temperature Data Logger (MTL).

Specifications of the data logger for the heat flow probe and the ANTARES Miniaturized Temperature Data Logger (MTL) are summarized below:

Heat Flow Data Logger DHF-650 (Kaiyo Denshi Co.)

Pressure case: titanium alloy
Case length: 725 mm
Maximum diameter: 145 mm
Pressure rating: 7000 m water depth
Number of temperature channels: 9
Temperature resolution: 1 mK
Tilt: two-axis, 0 to ±45°
Data-cycle interval: 30 sec
Pinger frequency: 15.0 kHz (or 12.0 kHz)

Miniaturized Temperature Data Logger (ANTARES Datensysteme GmbH)

Pressure case: stainless steel
Case length: 160 mm
Diameter: 15 mm
Pressure rating: 6000 m water depth
Number of temperature channel: 1
Temperature resolution: 1.2 mK at 20°C, 0.75 mK at 1°C
Sample rate: variable from 1 sec to 255 min.

[Operations]

A 15 m long nylon rope was inserted between the heat flow probe and the winch wire rope in order not to kink the wire rope during probe penetrations. An acoustic transponder and a pinger were attached about 40 m above the probe for precise determination of the position of the probe and the distance from the seafloor (Fig. 3.4-3).

Multi-penetration heat-flow measurement operations were conducted following the procedures described below.

1. Measure water temperature about 30 m above the seafloor for calibration of temperature recorders.
2. Lower the probe at a speed of about 1 m/sec until it penetrates into the sediment.
3. Measure temperatures in the sediment for about 15 min. Monitor the wire tension and pay out the wire when necessary to keep the probe stable.
4. Pull out the probe and move to the next station keeping the probe about 100 m above the seafloor.
5. Repeat penetrations.

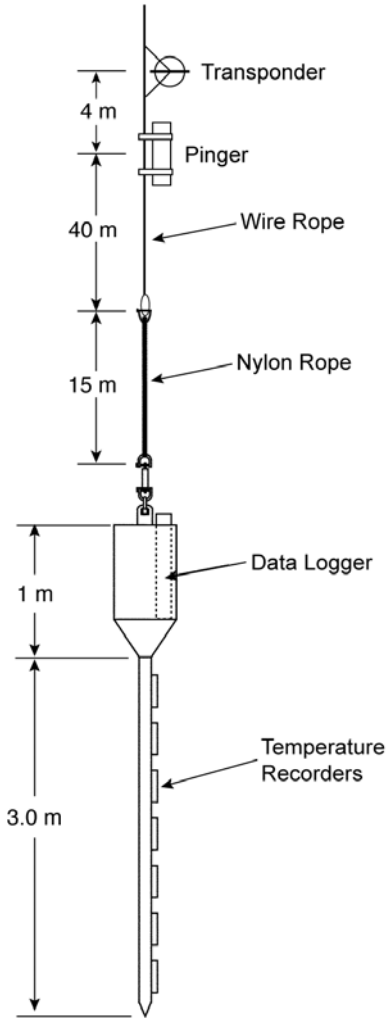

Figure 3.4-3. Configuration of the heat flow measurement system using a deep-sea probe.

3.4.2. Heat flow piston coring system

[Specification of tools]

During this cruise, sediment core samples were taken with the heat flow piston coring system (HFPC) (Fig. 3.4-4). This coring system was used for combined operation of measuring heat flow and recovering sediments. The general outline of the system is shown in Fig. 3.4-5.

A stainless steel barrel was attached to a piston core head of 800 kg weight. The core head has a space for mounting the heat flow data logger to record the temperatures of thermistor sensors mounted along the barrel. On this cruise, a violin-bow type sensor string was mounted on the outside of the barrel, between the base of the weight stand and the core catcher bit. A transponder was mounted on the winch wire to obtain the depth and position of this equipment. A pinger was also mounted on the winch wire to obtain the altitude from seafloor. The stainless steel barrel with this system is 4 m or 6 m in length and liner is used for recovering sediments.

The balance and pilot corer are the same as ones for ordinary piston core systems. 24 mm nylon rope was placed between the balance and winch wire for additional wire out and/or increased tension after hitting sea bottom. Because the system must be kept in the sediment for 15 to 20 minutes to obtain stable temperature, additional wire out is necessary for avoiding pulling the barrel out of the sea floor by either heaving or drifting of the ship during the measurement.

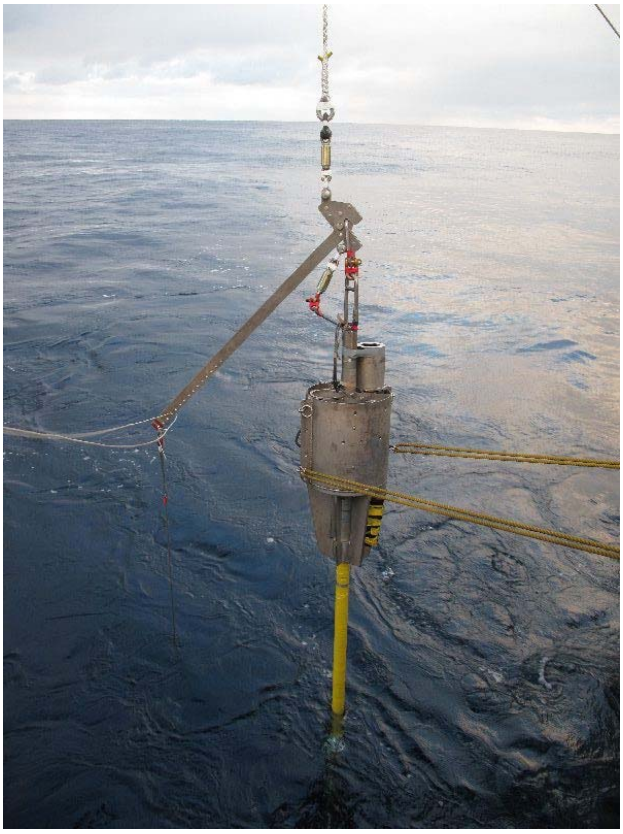

Figure 3.4-4. HFPC with temperature sensor string (violin-bow type).

[Operations]

Preparation for the piston coring

After barrels are attached to the head (weight stand), the main wire is connected, through the barrel, to the piston at the bottom of the barrel. The core catcher and bit are then attached. The balance is connected to the end of the main wire. The entire assemblage is carried under the A-frame using a cart and is lifted over the edge of the deck by the winch. A-frame and capstan winches, the pilot core and its wire are then connected to the balance. The system is then lowered through the water to the seafloor.

Hit the bottom and off the bottom

The piston core system starts lowering at a winch speed of 20 m/min, which gradually

increases to a maximum 60 m/min. The piston corer is stopped at a depth about 50 m above the seafloor for 10 minutes to reduce any pendulum motion and to calibrate the temperature sensors on the outside of barrel.

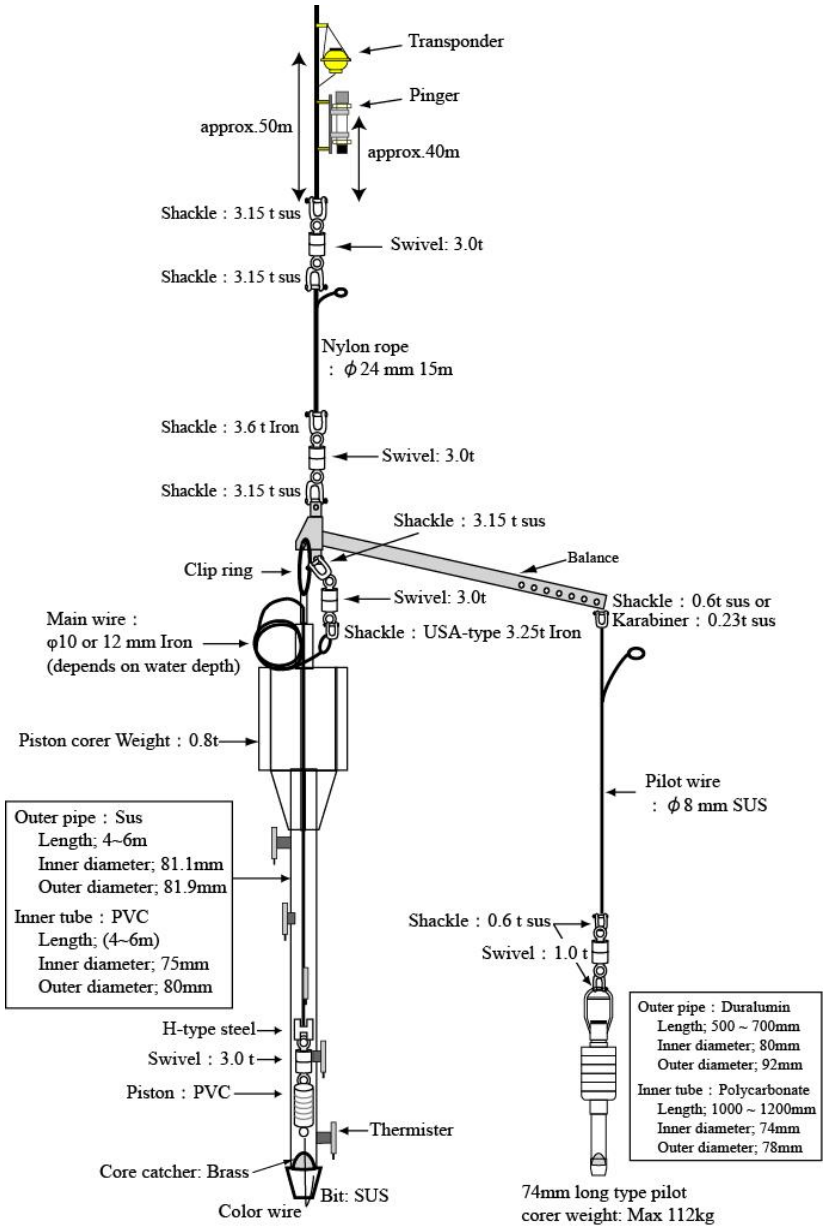

Figure 3.4-5. Configuration of the heat flow piston coring (HFPC) system.

After 10 minutes, the wire is lowered at a speed of about 20m/min., carefully watching the pen recorder of the strain gauge tension meter. When the piston corer hit the bottom the tension will abruptly decrease by the amount of the piston corer weight. Therefore, it is easy to detect the bottom hit.

After the recognition of the bottom hit, add 5 m to wire out, stop and keep the position for

15 ~ 20 minutes. And then, rewinding of the wire is started at a dead slow speed (~20 m/min.) until the tension gauge indicate that the corer has lifted off the bottom. The tension meter shows a small increase in tension when the corer is being pulled out of the seafloor and then a steady value. After we can recognize absolutely that the piston corer is above the seafloor, the winch speed is increased to 60 m/min., and then gradually to maximum speed.

3.4.3. Long-term temperature monitoring system

At stations with relatively shallow water depths (e.g., less than 2500 m), temporal variation of the bottom water temperature significantly disturbs the temperature profile in surface sediment, making it difficult to measure heat flow with ordinary deep-sea probes. One method to determine heat flow at such shallow sea stations is long-term monitoring of temperatures in surface sediment (Hamamoto et al., 2005). We can analytically remove the influence of the bottom water temperature variation from the long-term sediment temperature records. Another possible method is to conduct temperature profile measurement with a deep-sea probe after monitoring the bottom water temperature for a certain long period. We may be able to determine heat flow by analyzing the temperature profile combined with the water temperature record for the preceding period.

We have been using a pop-up water temperature measurement system (termed PWT below) in order to obtain long-term bottom water temperature records (Fig. 3.4-6). PWT consists of an acoustic releaser, weights, floats (glass spheres), and a small water temperature recorder (NWT-DN, Nichiyu Giken Kogyo Co.) (Fig. 3.4-7). For deployment, the whole system is released at the sea surface and it sinks freely down to the sea floor. The system is recovered by activating the acoustic releaser with a command sent from a surface ship.

Figure. 3.4-6. Pop-up water temperature measurement system (PWT).

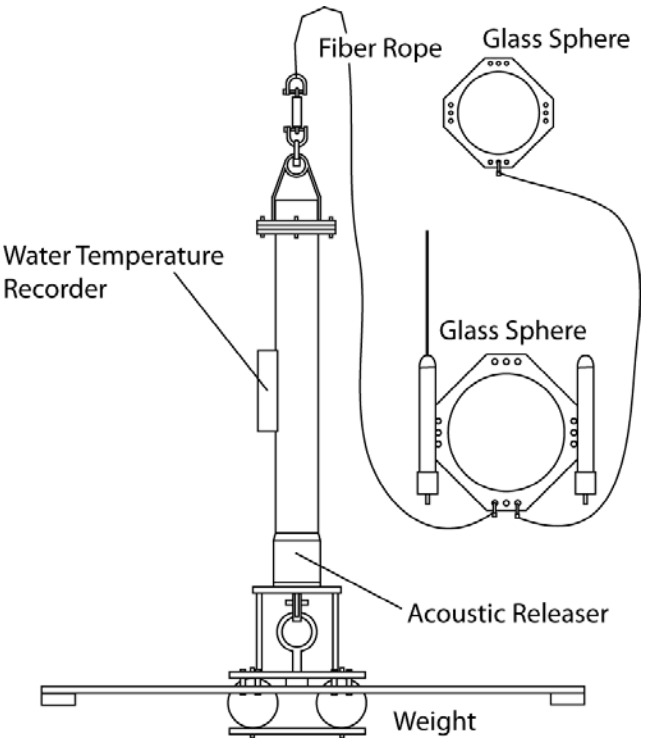

Figure 3.4-7. Schematic drawing of PWT.

Specifications of the water temperature recorder (NWT-DN) are summarized below.

Pressure case	titanium alloy
Case length	212 mm
Diameter	41 mm
Pressure rating	6000 m water depth
Number of temperature channel	1
Temperature resolution	1 mK
Sample rate	variable from 2 sec to 1 day

3.4.4. Physical properties of core samples

[Thermal property]

We need to know thermal conductivity of surface sediments in order to obtain heat flow values. Thermal conductivity of sediment core samples was measured using two different types of line-source commercial devices. One is QTM-500 (Kyoto Electronics Manufacturing Co.) with a half-space type box probe (Sass et al., 1984). The other is KD2 Pro (Decagon Devices) with a full-space type needle probe (von Herzen and Maxwell, 1959). KD2 Pro has the ability to measure thermal diffusivity (or heat capacity) as well as thermal conductivity by using dual-needle sensors (dual probes), while measurements with ordinary single-needle

sensors (single probes) give thermal conductivity only. We conducted measurements with these devices on split core samples.

[Magnetic susceptibility]

In order to know successive magnetic susceptibility throughout the whole-round piston cores, we used Magnetic Susceptibility Meter MS2 (Bartington Instruments) with a loop sensor. This measurement system was borrowed from Dr. Toshiya Kanamatsu (Institute for Research on Earth Evolution, JAMSTEC).

[Electrical resistivity]

In order to know electrical resistivity throughout the split core samples, we used a resistivity meter of four-pole method with a sensor (about 1 cm wide) equipped with four needles (about 0.5 cm long). This instrument was borrowed from Dr. Juichiro Ashi (Atmosphere and Ocean Research Institute, University of Tokyo). We penetrated the four needles into the split-core surface at 1 cm intervals and measured electric potential (mV). The obtained values will be converted into resistivity and porosity after the cruise.

[Shear strength]

In order to understand shear strengths of core samples under the undrainage and unconsolidation (UU) conditions, we conducted vane shear test. The shear strength is measured using four-wing-bearing torque driver of 2 cm in height and 1 cm in width. Measurements were made as follows; 1) the whole wings of the torque driver were penetrated directly into the split-core surface, 2) the torque driver was rotated slowly, 3) record the maximum torque force. The shear strength is calculated from the shear friction working during rotation of the driver as:

$$C = \frac{M_{t\max}}{\pi D^2 \left(\frac{H}{2} + \frac{D}{6} \right)}$$

where C is the shear strength (kg/cm^2), $M_{t\max}$ is the torque moment (kg cm), H is the wing height (cm), and D is the total wing width (cm).

3.4.5. Ocean-bottom electromagnetometer (OBEM)

[Type A OBEM]

The OBEM system (type A) was designed to investigate the crustal and mantle structure. This system consists of one 17-inch glass sphere, and then a high-accuracy fluxgate magnetometer is mounted outside the glass sphere (Fig. 3.4-8). Concepts of our developed

OBEM system are miniaturization, a high sampling rate, easy assembly and recovery operations, and low costs of construction and operation. It has a folding-arm system to facilitate assembly and recovery operations (Kasaya et al., 2006; Kasaya and Goto, 2009). Figure 3.4-9 shows the schematic diagram of the arm-folding system. For measuring the electric field, we used Ag-AgCl electrode mounted at the toe of each electrode arm. Electric circuit used for each system is contained in the pressure glass spheres. The fluxgate magnetometer of the OBEM system is mounted outside the glass sphere (Fig. 3.4-8). The salient characteristic of our system is its arm-folding mechanism, which facilitates and simplifies our onboard operations. We used an acoustic release system that had been already used by JAMSTEC for Ocean Bottom Seismography (OBS). Therefore, this acoustic system can communicate with the Kairei's SSBL system and it is easy for us to detect its position in the sea or on the seafloor. The acoustic code, the beacon frequency, and the electric dipole length are listed in Table 3.4-1.

Long continuous measurement with high sampling rate is ideal to estimate wide-band MT response. However, type A OBEM allows only 37 days measurement due to the limitation of battery size and memory when the sampling rate is settled to 8 Hz. Therefore, we modified one of the OBEM (JM100, site B13) for this cruse to change sampling rate during observation. The modification enables us to obtain wide-band MT responses if the sampling rate is switched to low after short-term measurement with high sampling rate. In this operation, we settled 8 Hz sampling rate for 24 days from the deployment and 60 sec sampling rate after that.

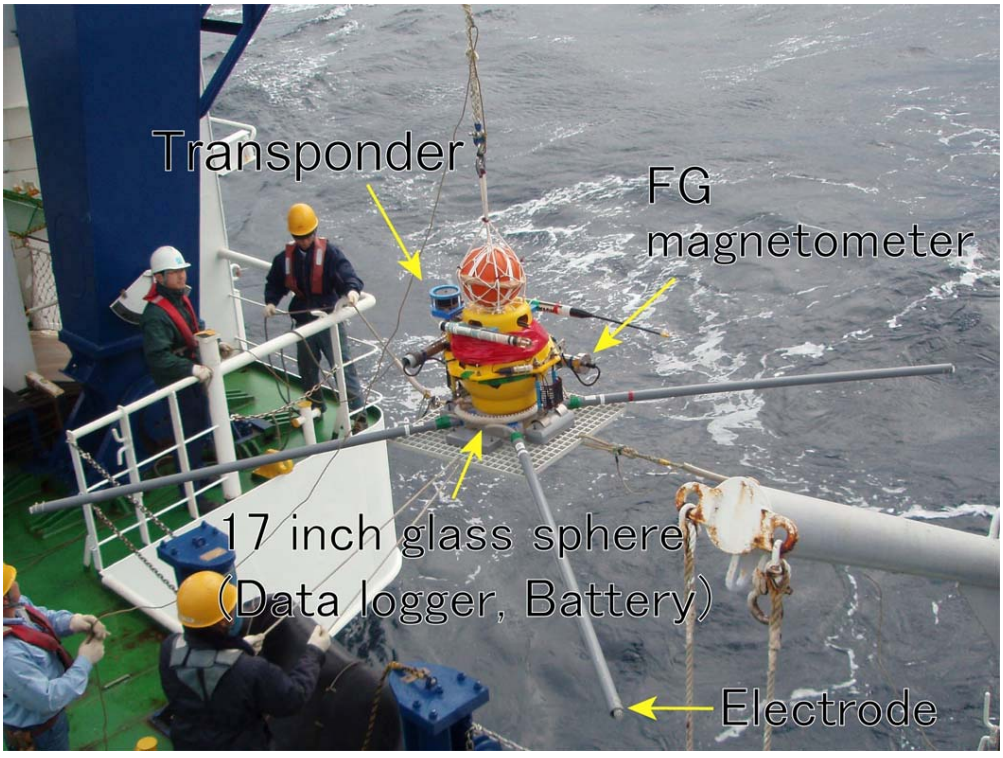

Figure 3.4-8. Photograph of type A OBEM.

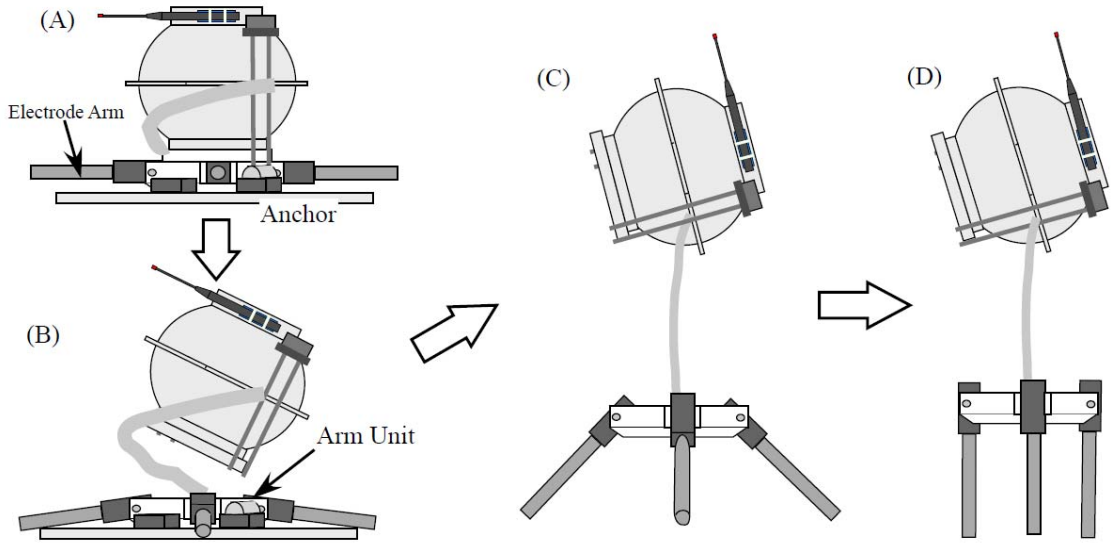

Figure 3.4-9. Schematic illustration of the arm-folding system of type A OBEM.

Table 3.4-1. Specification of OBEMs

Site ID	OBEM ID	OBEM Type	Dipole length (m)	Acoustic code	Beacon freq. (MHz)	Sampling rate (sec.)
C11	JM102	Type A	4.40/ 4.40	4D-1	43.528 (JS1364)	0.125
B11	JM103	Type A	4.40/4.40	4C-1	43.528 (JS1299)	0.125
B12	JM101	Type A	4.40/4.40	4E-1	43.528 (JS1368)	0.125
B13	JM100	Type A	4.40/4.40	2A-1	43.528 (JS1363)	0.125/60
B14	ERI14	Type B	5.37 / 5.37	4B-1	43.528 (JS190)	60

[Type B OBEM]

The type B OBEM (Fig. 3.4-10) is made by Tierra Technica, which can measure time variations of three components of magnetic field, horizontal electric field, the instrumental tilts, and temperature. The resolutions are 0.01 nT for flux-gate magnetometer, 1.19 nV for voltmeter, 0.00026 degrees for tiltmeter, and 0.01°C for thermometer. The type B OBEM is equipped with two glass spheres on a titanium frame. Each sphere houses the electromagneotmeter, and a Lithium battery pack and an acoustic transponder, respectively. A radio beacon, a flash light, and a catching buoy for easy recovery are mounted on the type B OBEM. For electric field, four voltage differences between the electrodes on the tip of the pipes and the ground electrode are measured. The electrodes are Ag-AgCl equilibrium type made by Clover Tech. The acoustic code, the beacon frequency, and the electric dipole length

are listed in Table 3.4-1. The electrodes were monitored their self-potentials in laboratory in advance of the seafloor observation and pairs that the coherence is high enough were selected, in order to reduce the noise due to the voltage drift of electrodes themselves (Fig. 3.4-11).

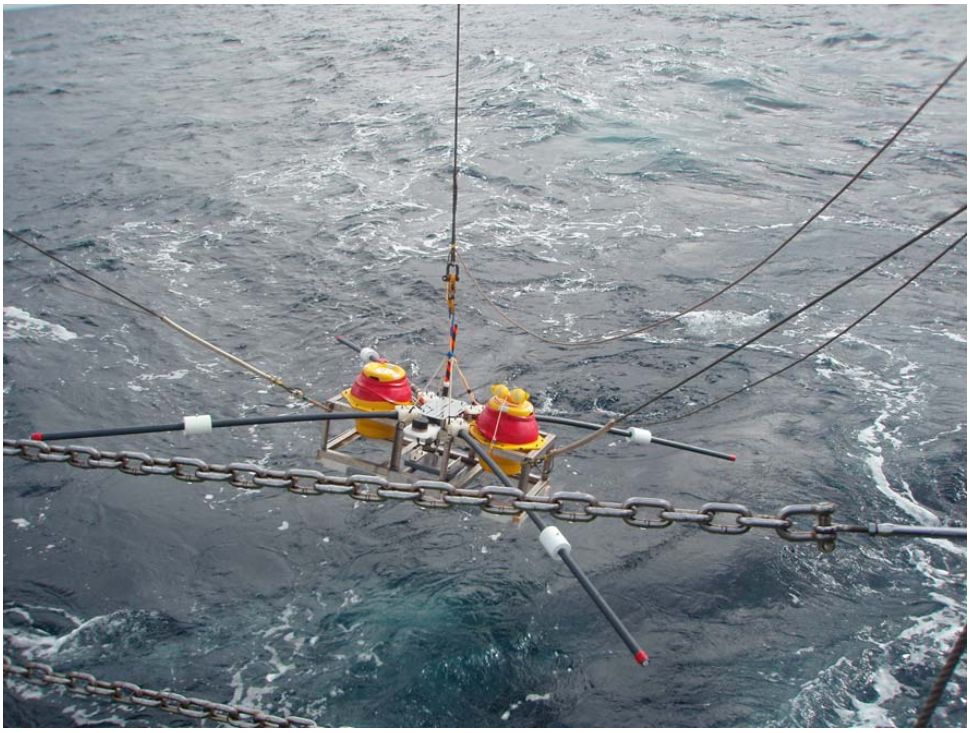

Figure 3.4-10. Photograph of type B OBEM.

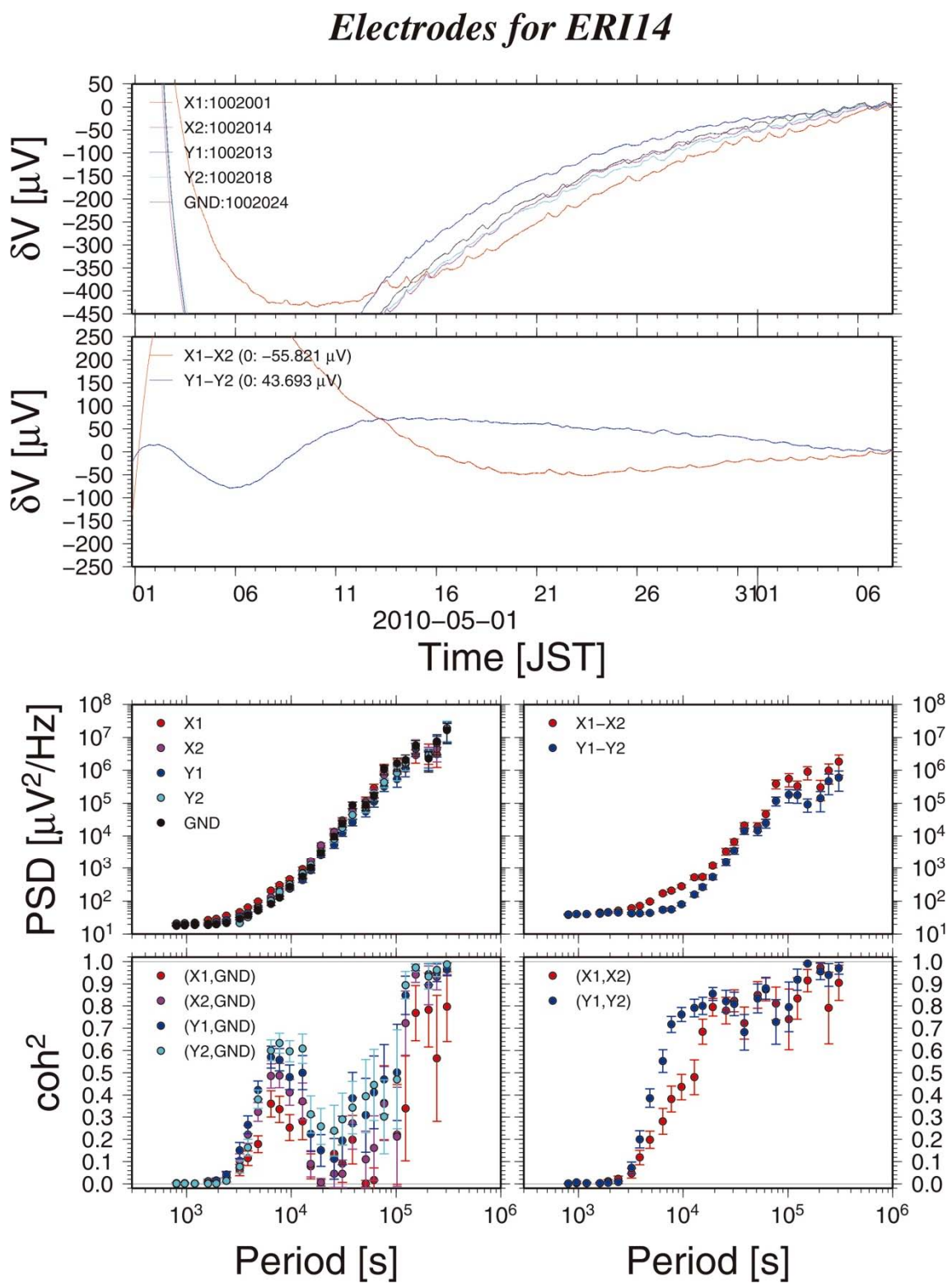

Figure 3.4-11. Self-potentials of the electrodes monitored in laboratory, and their power.

3.5. Preliminary Results

3.5.1. Heat flow measurement

We carried out heat flow measurements at seven sites with the deep-sea heat flow probe and at three sites with the HFPC (Table 3.5-1; Fig. 3.2-2). At all the sites with the deep-sea heat flow probe, multiple penetrations were made for examining local variability of heat flow. The coordinates of the stations listed in Table 3.5-1 are the positions of the acoustic transponder attached just above the probe or HFPC determined with the SSBL system of the ship, though the position of the ship is shown for HF01 and HFPC01 because the transponder was broken or was not used during the measurements at these sites. The water depth in the table is the depth right below the ship determined with the multi-narrow beam echo sounder and may be slightly different from the depth at the station.

Most of the sites are located seaward side of the Japan Trench along the survey lines A and B (cf. Fig. 3.3-2), while site HFPC03 is on the landward slope of the trench. At HFPC01, close to the OBEM B14, the piston corer fell down about two minutes after the penetration probably due to insufficient penetration depth, and temperature profile data could not be obtained. The core sample at HFPC01 contains thick volcanic ash layers (cf. 3.5.3), which may have prevented deep penetration of the core barrel. At HF04 and HF05, the temperature records indicate peculiar two-step penetration of the probe: the probe penetrated to some depth when it hit the bottom and moved further downward one to four minutes after the first penetration. The unusual movement of the probe was possibly caused by volcanic ash layer(s), which could have acted as a barrier to the first penetration and have then failed a couple of minutes later.

Sites HF03, HF06, HF07 and HFPC02 are located on the trench outer rise and to the east of the heat flow measurements in the last three-year survey. Results at these sites provide information on the seaward limit of the high heat flow. At Sites HF01, HF02, HF04 and HF05, located on the western slope of the outer rise, we conducted closely-spaced measurements in the vicinities of stations where very high heat flow had been observed in order to examine the detailed heat flow distribution around a local high anomaly.

Heat flow values will be obtained by combining the measured temperature profiles with thermal conductivity of surface sediment. Thermal conductivity at each site needs to be estimated from the values measured on piston core samples (cf. 3.5.3) and the existing data at nearby stations.

Table 3.5-1. Results of heat flow measurements

Date	Station	Latitude (N)	Longitude (E)	Depth (m)	N
Deep-sea heat flow probe					
Nov. 17	HF01A*	38°59.88'	145°07.11'	5485	4
	B*	38°59.85'	145°06.87'	5485	4
Nov. 19	HF02A	40°14.08'	145°40.56'	5200	6
	B	40°14.29'	145°40.55'	5210	6
	C	40°14.57'	145°40.63'	5215	7
	D	40°14.81'	145°40.52'	5215	7
	E	40°15.05'	145°40.53'	5215	6
	F	40°15.21'	145°40.57'	5220	7
	G	40°15.36'	145°40.59'	5215	6
Nov. 20	HF03A	38°46.51'	146°42.94'	5245	7
	B	38°46.51'	146°43.00'	5245	7
	C	38°46.53'	146°43.27'	5245	6
Nov. 21	HF04A	38°59.89'	145°04.96'	5480	5
	B	38°59.90'	145°05.18'	5480	4
	C	38°59.88'	145°05.49'	5485	4
	HF05A	38°59.69'	145°08.94'	5475	6
	B	38°59.73'	145°09.09'	5470	4
	C	38°59.70'	145°09.24'	5470	7
Nov. 22	HF06A	40°15.03'	146°55.01'	5315	6
	B	40°14.98'	146°55.42'	5310	7
	HF07A	40°15.05'	146°39.98'	5290	6
	B	40°14.82'	146°40.18'	5290	7
HFPC					
Nov. 17	HFPC01*	39°02.04'	144°48.55'	5810	fell
Nov. 20	HFPC02	38°43.99'	147°03.97'	5410	6
Nov. 27	HFPC03	39°08.61'	143°39.59'	3730	6

N: number of temperature sensors used to obtain temperature profile in sediment.

*: position of the ship.

3.5.2. Long-term temperature monitoring

We recovered one pop-up water temperature measurement system (PWT; cf. 3.4.3) at a station off the Boso Peninsula, PWT1 (Table 3.5-2; Fig. 3.2-3). The system was deployed in August 2009 during KR09-10 cruise. The water temperature recorder (NWT-DN) yielded bottom water temperature data of good quality for 14 months (Fig. 3.5-1). This long-term record will be analyzed in combination with sediment temperature profiles measured in August 2009 and June 2010 to estimate heat flow at this site.

Table 3.5-2. Recovery of long-term temperature monitoring instrument

Station	Deployment	Recovery	Coordinates	Water depth (m)
PWT1	Aug. 15, 2009	Nov. 14, 2010	34°42.6'N, 140°28.9'E	2050

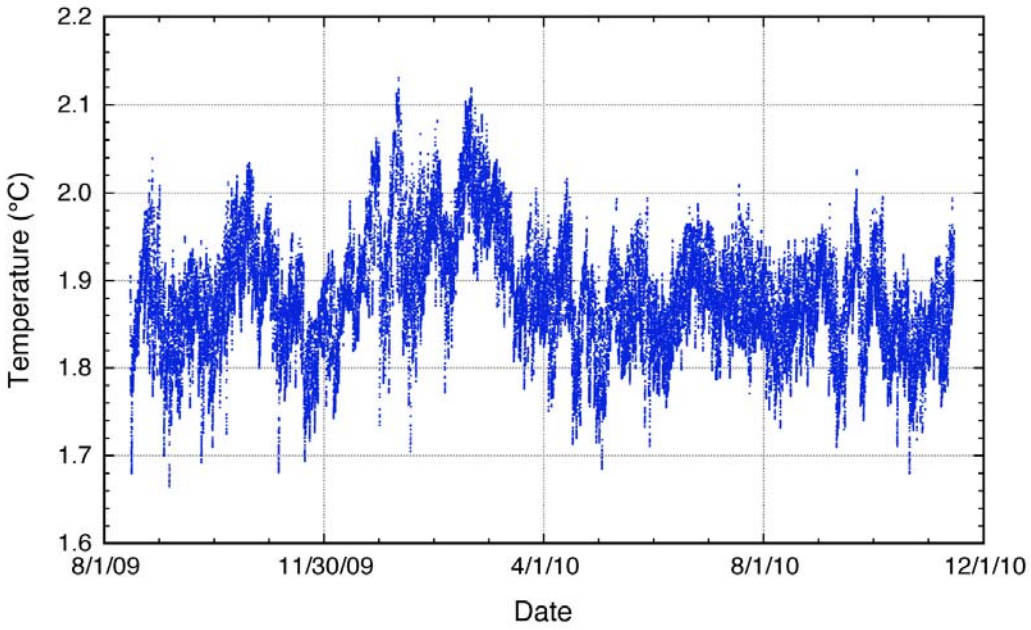

Figure 3.5-1. Bottom water temperature record at PWT1.

3.5.3. Piston core samples

Piston core samples were collected at three sites off Miyako, northeast Japan using 4-m and 6-m piston-corer systems operated by Marine Works Japan Co. Ltd. The piston corer system has a pilot corer (so-called a Marine Work Gravity Corer), so that a piston core sample and a pilot core sample were collected from one coring site. A sensor string with eight temperature sensors was attached along the core barrel of the piston corer for heat flow measurement. We call this system a heat-flow piston corer (hereafter HFPC). Sample names of the piston cores

and pilot cores are KR10-12 HFPC01, 02, 03 and HFPL01, 02, 03 in this description, respectively. But official sample names for curation at the Kochi Core Center are KR10-12 PC01, 02, 03 and PL01, 02, 03.

The piston core and pilot core samples were processed as follows;

1) Cut the whole core into 1-m sections.
2) Measure magnetic susceptibility at 2 cm intervals (i.e. 1, 3, …. 97, 99 cm) using Bartington MS-2 system with a loop sensor (cf. 3.4.4).
3) Sample about 30-cm long whole-round core from muddy sediments (inferred from magnetic susceptibility data) for physical property measurement at the Kochi Core Center.
4) Split the whole core into WORKING half and ARCHIVE half.
5) ARICHIVE half: describe sedimentary structures by naked eyes and smear slides.
6) Take photographs.
7) Take samples successively for geochemical studies.
8) WORKING half: Measure thermal conductivity using a box probe and needle probes (cf. 3.4.4).
9) Measure shear strength and electrical resistivity of the core samples using a vane shear tester and a resistivity meter (cf. 3.4.4).
10) Take samples successively for physical and magnetic properties measurements using 7-cc-plastic-cubes.
11) Pack cores into D-tubes, then transport to the Kochi Core Center.

It should be noted that WORKING half of the HFPC03 was replaced with ARCHIVE half, because of a problem in core splitting.

The recovered three core samples are described in detail below.

[HFPC01 and HFPL01]

To measure heat flow along the multi-channel survey line, HFPC01 was conducted on a flat surface in a graven along the Japan Trench at 39°02.04’N and 144°48.55’E. The water depth was 5808 m. Although parallel continuous layer structures were observed to a depth of at least 20 m in a subbottom profiler image to the south of the coring site, we could not make coring operation there due to an unexpected accident. Then, we moved to the coring site three nautical miles north of the original site.

We used the 6-m-piston coring system. When the corer was hit on the seabed, it fell down after about two minutes. We immediately pulled the corer out of the seabed, and recovered the coring system. The core barrel was bent by about 40 degrees at about 130 cm from the core bit. We cut the barrel into about 50-cm long sections using a band saw and pulled out inner pipes from the barrel. Finally the core was divided into nine small sections: Sections 1, 2-1, 2-2-1,

2-2-2, 2-3-1, 2-3-2, 3-1, 3-2 and core catcher (hereafter CC).

The recovered piston and pilot cores are 244 cm and 50 cm long, respectively. However, we suppose that the piston core is elongated at three horizons as follows.

1) Surface layer of Section 1: Based on the sedimentary structures in the pilot core, Section 1 should be 12 cm long, although the length of the recovered core is 23 cm. Top of Section 2 should be 12 cm below the seafloor (hereafter cm-bsf).
2) Volcanic ash layer at 20-44 cm in Section 3-1: Based on the volume reduction of the ash layer, we estimated that the original thickness should be one third of the elongated thickness. We changed the thickness of the volcanic ash layer from 24 cm to 8 cm on the basis of the above estimation.
3) Flow-in sediments from 47 cm in Section 3-2 throughout to CC.

Hence, we interpreted that the original core length was 181 cm before elongation. This inference is consistent with the penetration depth estimated from temperature data. We use this original core length (reconstruction) in the following core description.

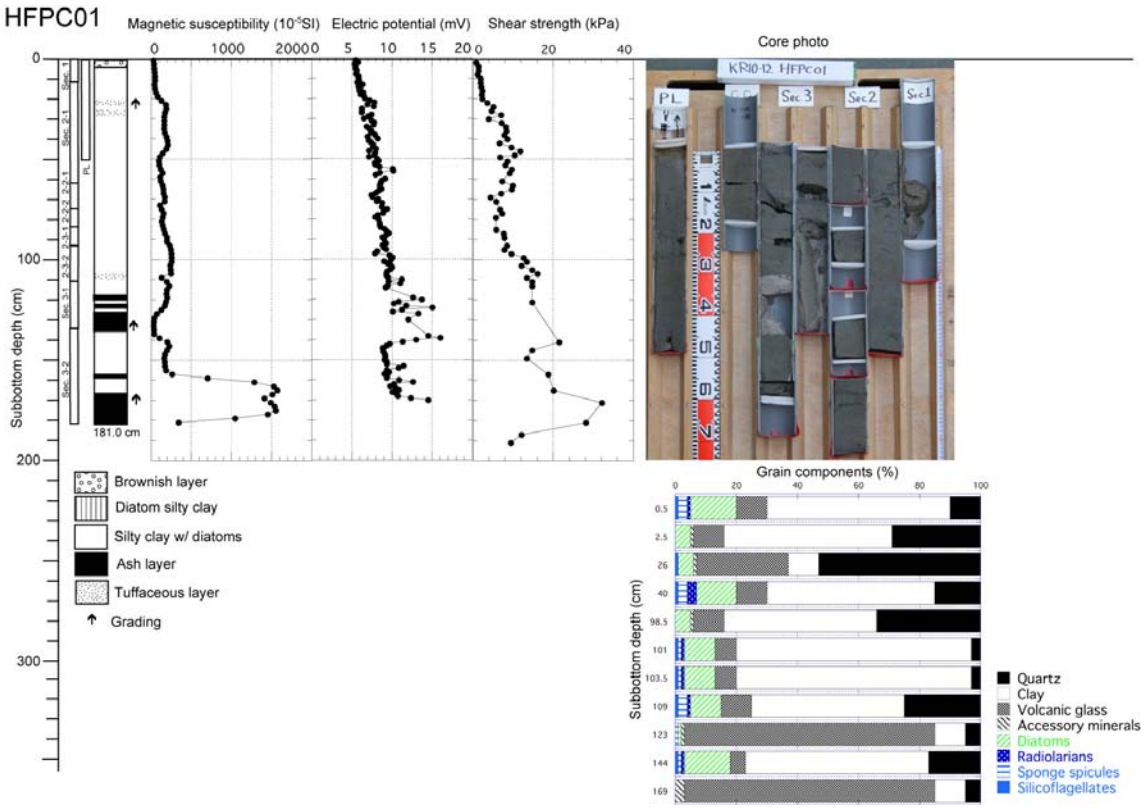

Figure 3.5-2. Summary of HFPC01.

The core sediment is predominantly olive black (10Y3/2) silty clay with diatoms, which is composed of mostly siliciclastic grains, diatoms, volcanic glass and clay particles. The silty

clay has pyritized burrows filled with grayish mud in places. Grayish volcanic ash layers are seen at 126-137, 158-159 and 167-181 cm-bsf. Erosional surfaces are seen at 24 and 27 cm-bsf.

Magnetic susceptibility is mostly 2 x 10^{-3} SI. The volcanic ash layer at 126-137 cm-bsf has low susceptibility, whereas susceptibility in the layer at 167-181 cm-bsf is high. Electric potential (mV) changes from 5.0 to 10.0 throughout the core. It means that the water content decreases with increase of burial depth. Shear strength in silty clay increases progressively from about 0 to about 20 kPa with increase of burial depth, and it increases drastically in the volcanic ash layers.

Thermal conductivities of sediments were measured with QTM-500 at 10 locations on split core samples of HFPC01 and 4 locations on split core samples of HFPL01. Thermal conductivities of sediments were also measured with KD2 Pro with single probes at 11 locations on the HFPC01 core samples and 4 locations on the HFPL01 core samples. The measurement points are the same as those measured with QTM-500, except for one location. With KD2 Pro with dual probes, thermal properties (thermal conductivity, heat capacity and thermal diffusivity) were measured at the same locations as those measured with KD2 Pro with single probes.

[HFPC02 and HFPL02]

To measure heat flow along the multi-channel survey line, HFPC02 was conducted on the outer rise of the Japan Trench at 38°43.99'N and 147°03.97'E. The water depth was 5411 m. We used the 4-m piston coring system.

The recovered piston and pilot cores are 336 cm and 62 cm long, respectively. The piston core sediments are predominantly olive black (7.5Y3/2) silty clay including many volcanic glasses as hemipelagic clayey sediments. Five gray (7.5Y6/1) to grayish olive (7.5Y4/2) volcanic ash layers are seen at 98-105, 129-130, 141-144, 180-181 and 206-208 cm-bsf. Volcanic ash rich layers of pale color are seen at 74-80, 130-137, 197-201, 229-233 and 259-288 cm-bsf.

Magnetic susceptibility of the silty clay is 1-2 x 10^{-3} SI. Electric potential increases from ~5 to 10 mV within ~150 cm burial depth, and it fluctuates around 10 mV below 150 cm-bsf. Shear strength increases successively with increase of depth to about 20 kPa at ~150 cm-bsf, whereas it fluctuates around 20 kPa below 150 cm-bsf.

Thermal conductivities of sediments were measured with QTM-500 at 14 locations for HFPC02 core samples and 4 locations for HFPL02 core samples. Thermal conductivities of core samples were also measured with KD2 Pro with single probes. With KD2 Pro with dual probes, thermal properties (thermal conductivity, heat capacity and thermal diffusivity) were

measured. The measurement locations with KD2 Pro with both single and dual probes are the same as those measured with QTM-500.

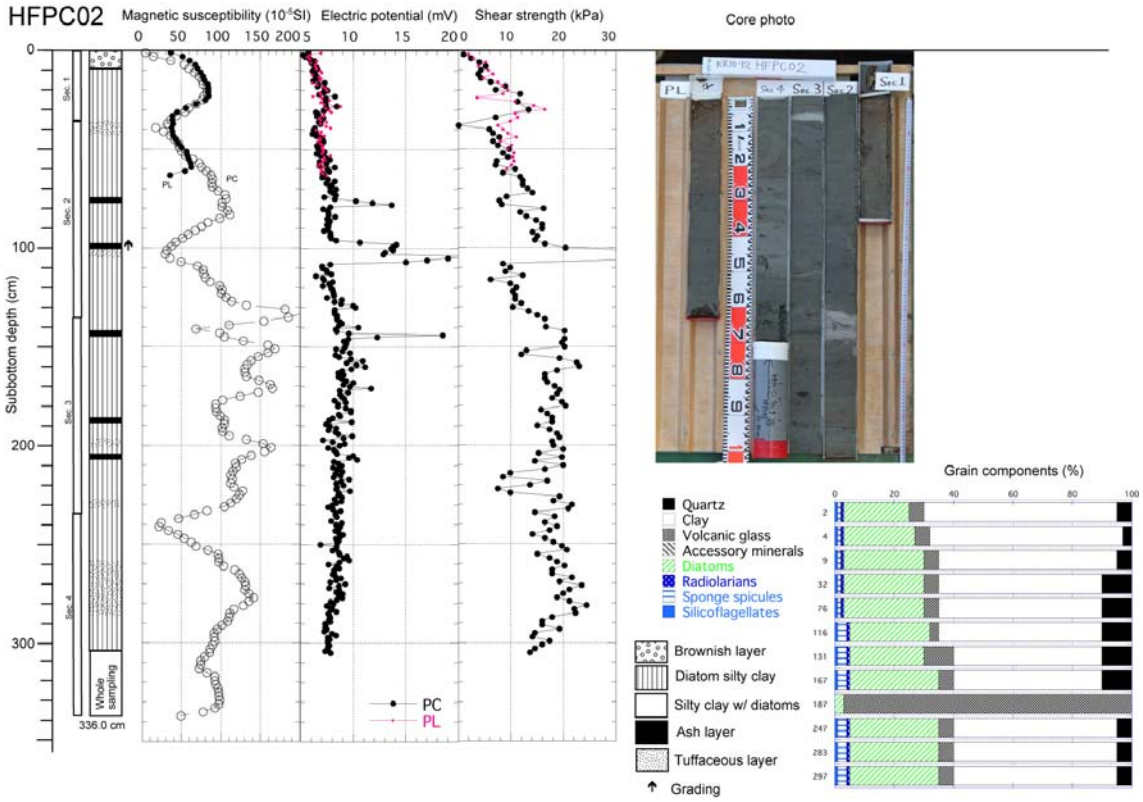

Figure 3.5-3. Summary of HFPC02.

[HFPC03 and HFPL03]

To measure heat flow along the multi-channel survey line, HFPC03 was conducted on a gentle slope on the landward trench slope at 39°08.61'N and 143°39.59'E. The water depth was 3725 m. We found layering structures of about 20 m thick and a strong reflector just below the layering structures with the subbottom profiler system.

The piston and pilot cores are 155 cm and 54 cm long, respectively. But the upper part of the piston core should be reconstructed for the following reasons. There are two magnetic susceptibility (hereafter MS) peaks in HFPC and HFPL cores. The horizon of the lower MS peaks in HFPC is mostly same as that in HFPL at about 45 cm-bsf, whereas the horizons of upper MS peaks are quite different, 30 cm-bsf in HFPC and 10 cm-bsf in HFPL. We interpreted this difference as a result of compression in the upper layer from top to about 45 cm-bsf (just above the lower MS peak) in HFPC. Therefore, we reconstructed the original lithological unit using two cores, PL and PC. The reconstructed unit is composed of two layers: PL above the lower MS peak and PC below the peak. We use the reconstructed unit in the description below.

The major lithology of HFPC03 is olive black (7.5Y3/2) diatom silty clay. Three volcanic ash layers are seen at 18-19, 45-46 and 143-145 cm-bsf. We found color changes from lighter to darker at 58, 74, 101, 113 and 143 cm-bsf. The darker color layer corresponds to diatom-rich layer, whereas the lighter color layer is diatom-poor layer being silty clay with diatoms.

Magnetic susceptibility of the silty clay is 1 x 10^{-3} to 1 x 10^{-4} SI. Electric potential increases from ~5 to 10 mV with increase of burial depth. Shear strength increases successively to about 10 kPa throughout the core.

Thermal conductivities of sediments were measured with QTM-500 at 7 locations for HFPC03 core samples and 4 locations for HFPL03 core samples. Thermal conductivities of core samples were also measured with KD2 Pro with single probes. With KD2 Pro with dual probes, thermal properties (thermal conductivity, heat capacity and thermal diffusivity) were measured. The measurement locations with KD2 Pro with both single and dual probes are the same as those measured with QTM-500.

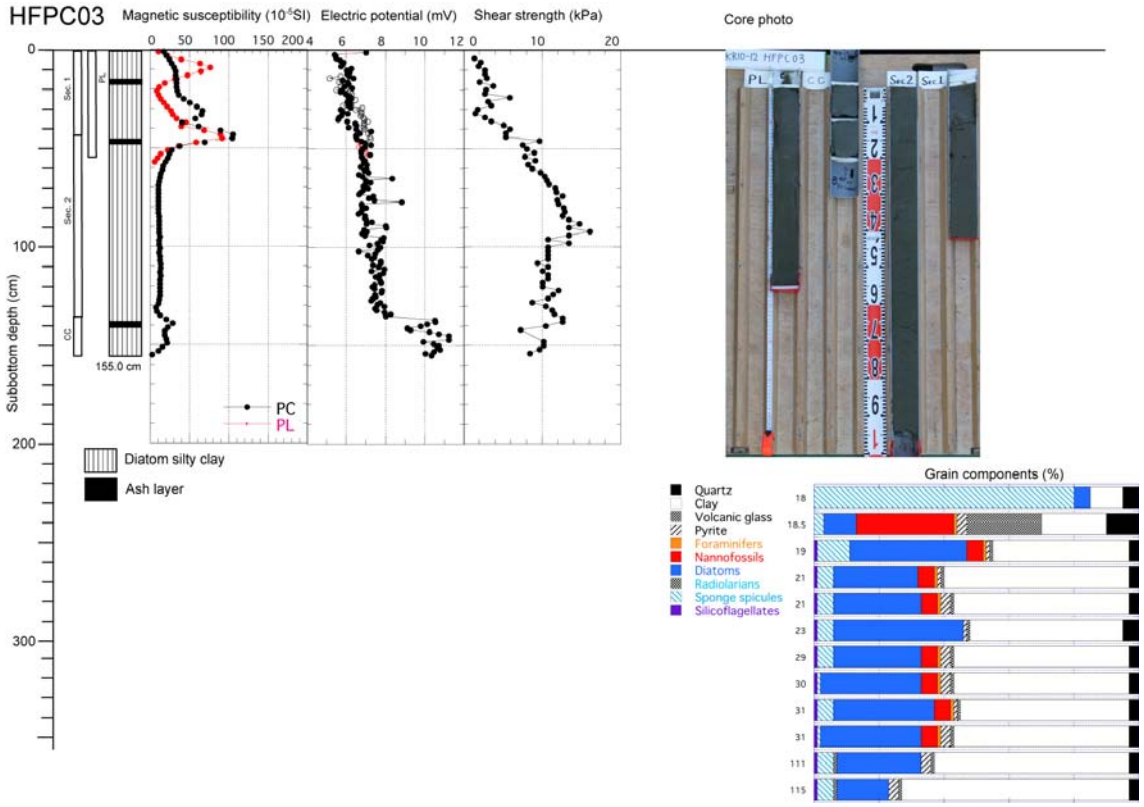

Figure 3.5-4. Summary of HFPC03.

3.5.4. Electromagnetic survey

[Deployment of OBEMs]

We successfully deployed four type A OBEMs (JM100, JM101, JM012, JM103) and one type B OBEM (ERI14) in this cruse (Fig. 3.3-4). The specifications of each OBEM are shown in Table 3.4-1. Three type A OBEMs (JM101, JM102, JM103) were planned to be recovered in this cruse. In order to obtain high quality data in this short measurement period, they were deployed in a relatively shallow sea area (<900m) where attenuation of the signal is low (sites B11, B12, C11 in Fig. 3.3-4). The measurements were started before the settlement with 8-Hz sampling rate. The other two OBEMs (JM100 [type A], ERI14 [type B]) will be recovered more than five months after. The sampling rate of ERI14 is settled to 60 s to obtain low frequency MT/GDS responses. For the other OBEM (JM100), we settled 8-Hz sampling rate for 24 days from the deployment and 60-s sampling rate after that in order to obtain wide-band MT/GDS responses. We could track the positions of the OBEMs by SSBL system of R/V Kairei because the communication frequency of our acoustic system matched the SSBL system. The settling rates were 41-46 m/min for type A OBEMs and 39 m/min for type B OBEM. Landing position of each OBEM was determined by SSBL system (Fig. 3.5-5; Table 3-5.3).

Clock synchronization before deployment and calibration after recovery is important. The OBEM system can synchronize to the laptop PC using USB communication. The laptop PC was synchronized with the NTP server unit connected to GPS immediately before setting of the OBEM system.

[Recovery of OBEMs]

We successfully recovered three type A OBEMs (site B11, B12, C11) without any trouble. They started ascending within about 15 minutes after sending the acoustic weight-release signal. Slant range between the ship and OBEM and ship's position were measured during ascending and ascent rate was calculated (Table 3.5-4). The estimated ascending rates (48-58 m/min) were faster than the average reported by Kasaya and Goto (2009). By tracking OBEM, its surface time was accurately predicted. OBEM was found with the ship looking into the direction of radio beacon signal and tracked position soon after the surfacing. The OBEMs were hooked from starboard deck and lifted on deck.

All OBEMs recorded data for full time of the observation periods. The clock of each OBEM was compared with the laptop PC synchronized by NTP server immediately after the recovery. The time difference between them for each OBEM is listed in Table 3.4-5. Raw time series data of all OBEMs show very good quality for electric and magnetic fields.

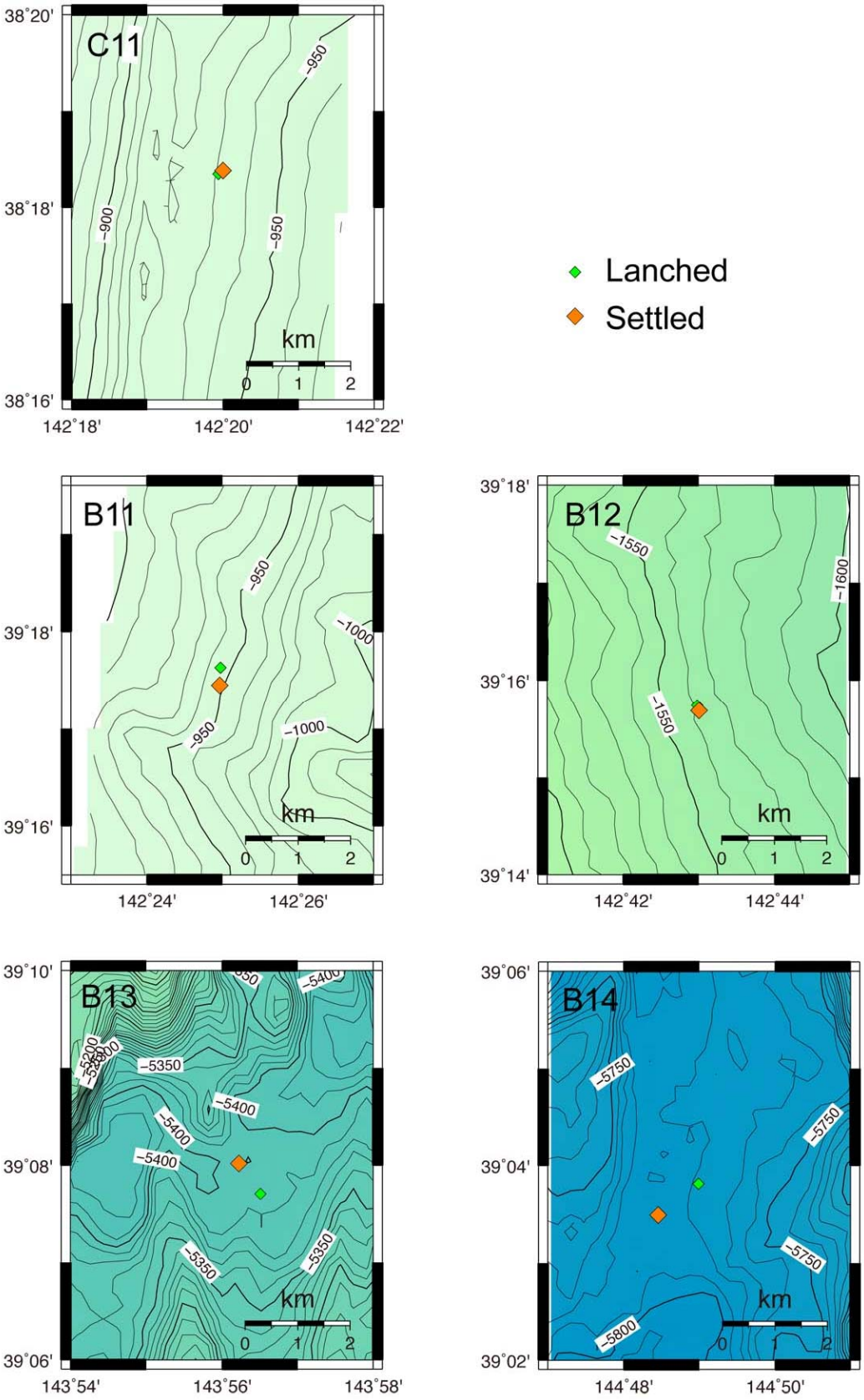

Figure 3.5-5. Detailed bathymetric maps around the launched and settled positions of the OBEMs.

Table 3.5-3. Launched and settled positions of OBEMs

Site ID	OBEM ID	Date	launched time (JST)	settled time (JST)	settled position		settled depth (m)
C11	JM102	2010/11/15	8:04	8:27	38:18.3814N	142:20.0027E	960.2
B11	JM103	2010/11/15	14:23	14:45	39:17.4501N	142:24.9657E	953.2
B12	JM101	2010/11/15	16:17	16:55	39:15.6863N	142:43.0074E	1558.5
B13	JM100	2010/11/16	6:46	8:45	39:08.0200N	143:56.2270E	5417.9
B14	ERI14	2010/11/16	12:22	14:50	39:03.4928N	144:48.4557E	5830.2

Table 3.5-4. Recovery information

Site ID	OBEM ID	On deck time (JST)	Ascent rate	Clock set time (JST)	Clock compare time (JST)	Time difference (sec)
C11	JM102	2010/11/26 13:19	48-58 (m/min)	2010/11/15 7:42	2010/11/26 13:34	+1.263
B11	JM103	2010/11/26 8:39	52.5 (m/min)	2010/11/15 13:37	2010/11/26 8:49	+0.593
B12	JM101	2010/11/26 6:42	52.6 (m/min)	2010/11/15 16:06	2010/11/26 7:07	+1.354

[OBEM data]

Raw time series of the OBEM data seem to show very high S/N for all sites (Figs. 3.5-6, 7, 8). However, variation of electric field of site B12 with long period exceeding 3 mV is very high as the variation due to induction phenomena. It may be caused by instability of electrode, tilt or seawater current. Magnetic variations corresponding to tilt variation are also recognized. In order to avoid effect of tilt variation, we conducted tilt correction for magnetic and electric field. Then we corrected time difference of OBEMs listed in Table 3.5-4. The azimuth showing maximum magnetic field was determined as the magnetic north of the OBEMs as listed in Table 3.5-5.

The time and tilt corrected time series of site B12 is shown in Figure 3.5-9. The corrected magnetic field shows obvious diurnal variations from Dec. 17 to Dec. 20. On the other hand, short period magnetic variations are also recognized after Dec. 22. Because these periods correspond to relatively high K-index periods (< 3) in Kakioka Geomagnetic Observatory, it seems to indicate true geomagnetic variation. Thus high-quality GDS/MT responses are expected to be obtained after remote reference processing and robust estimation techniques.

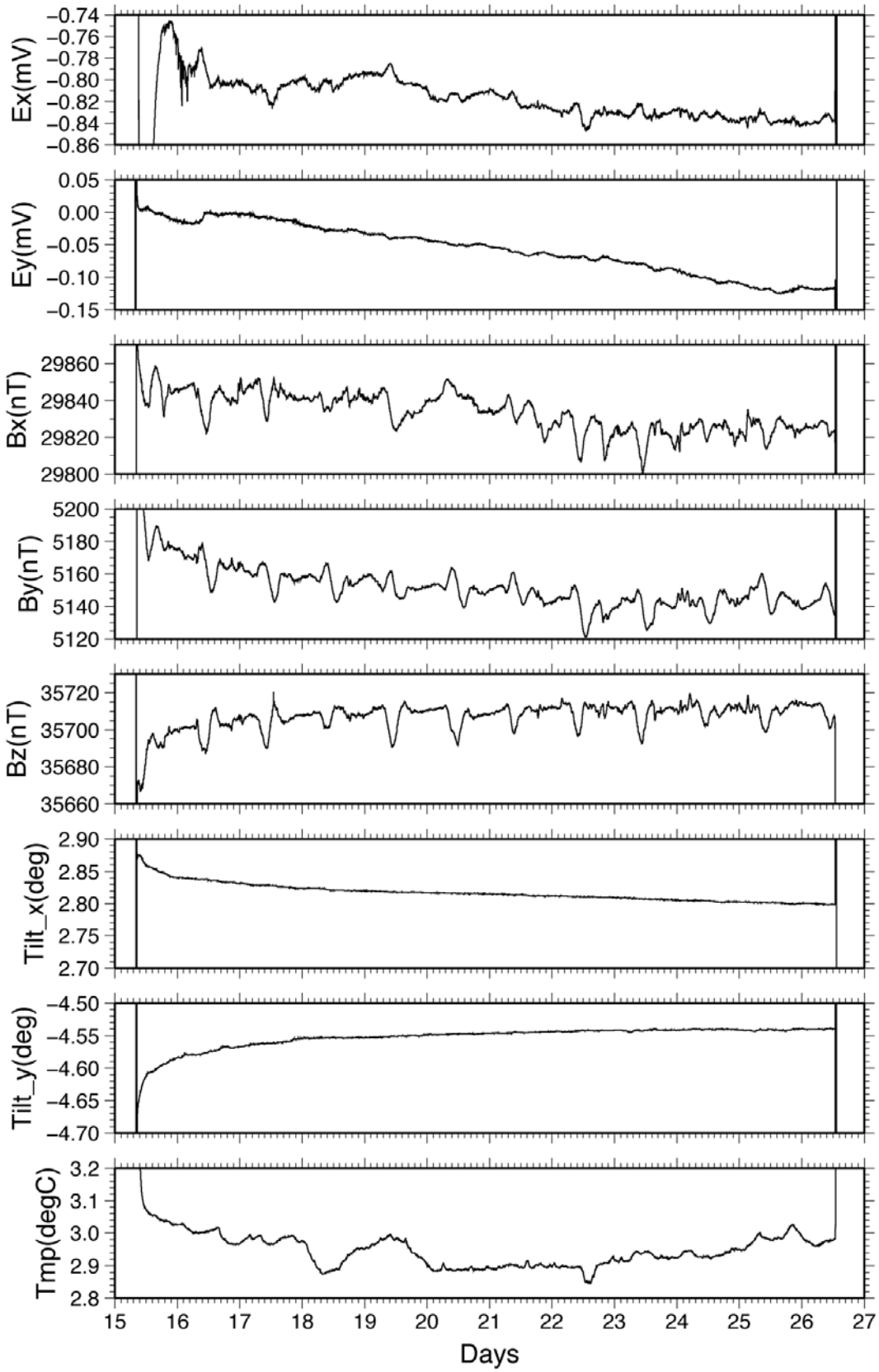

Figure 3.5-6. Raw time series at site C11 (in JST).

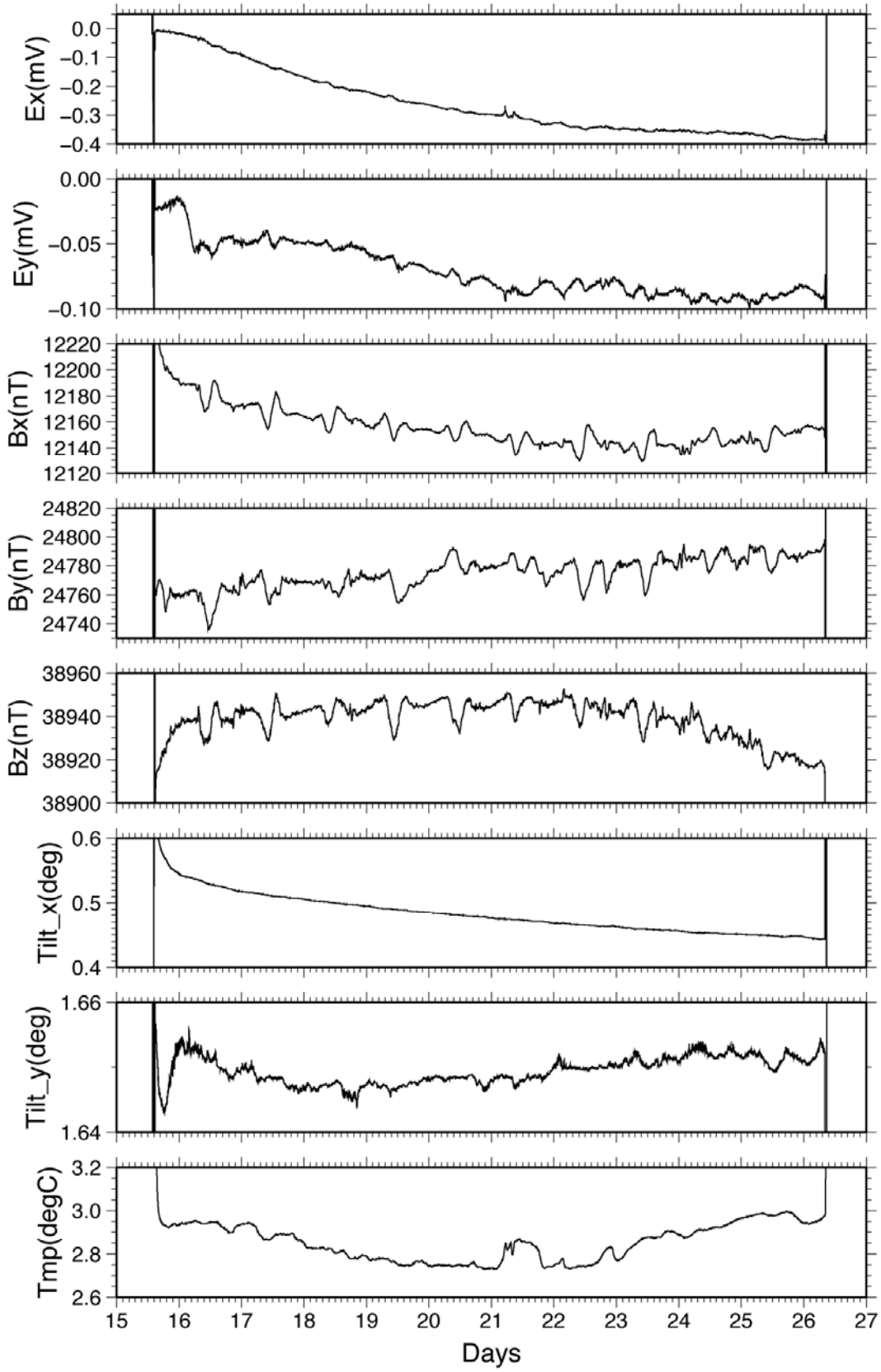

Figure 3.5-7. Raw time series at site B11 (in JST).

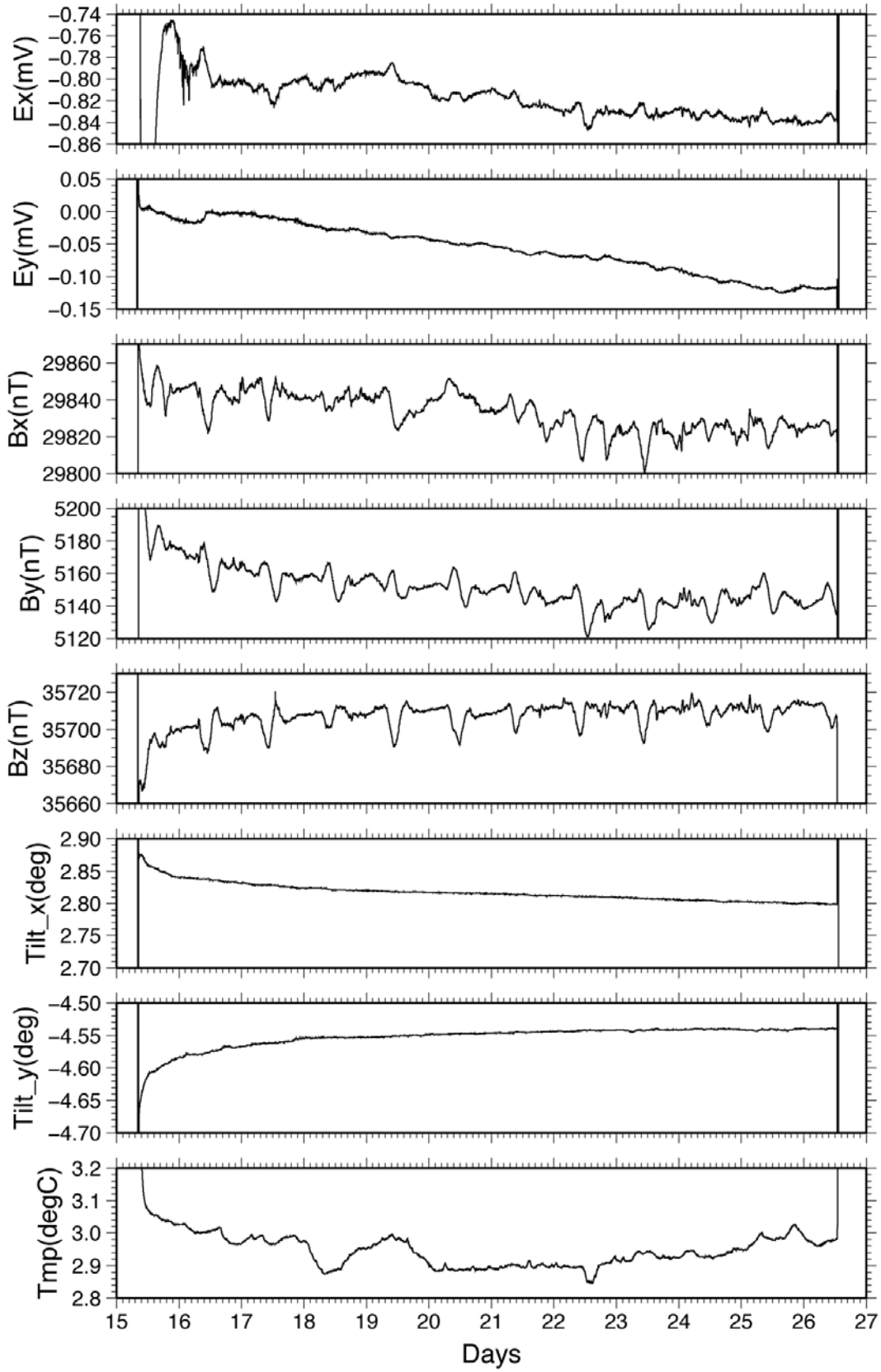

Figure 3.5-8. Raw time series at site B12 (in JST).

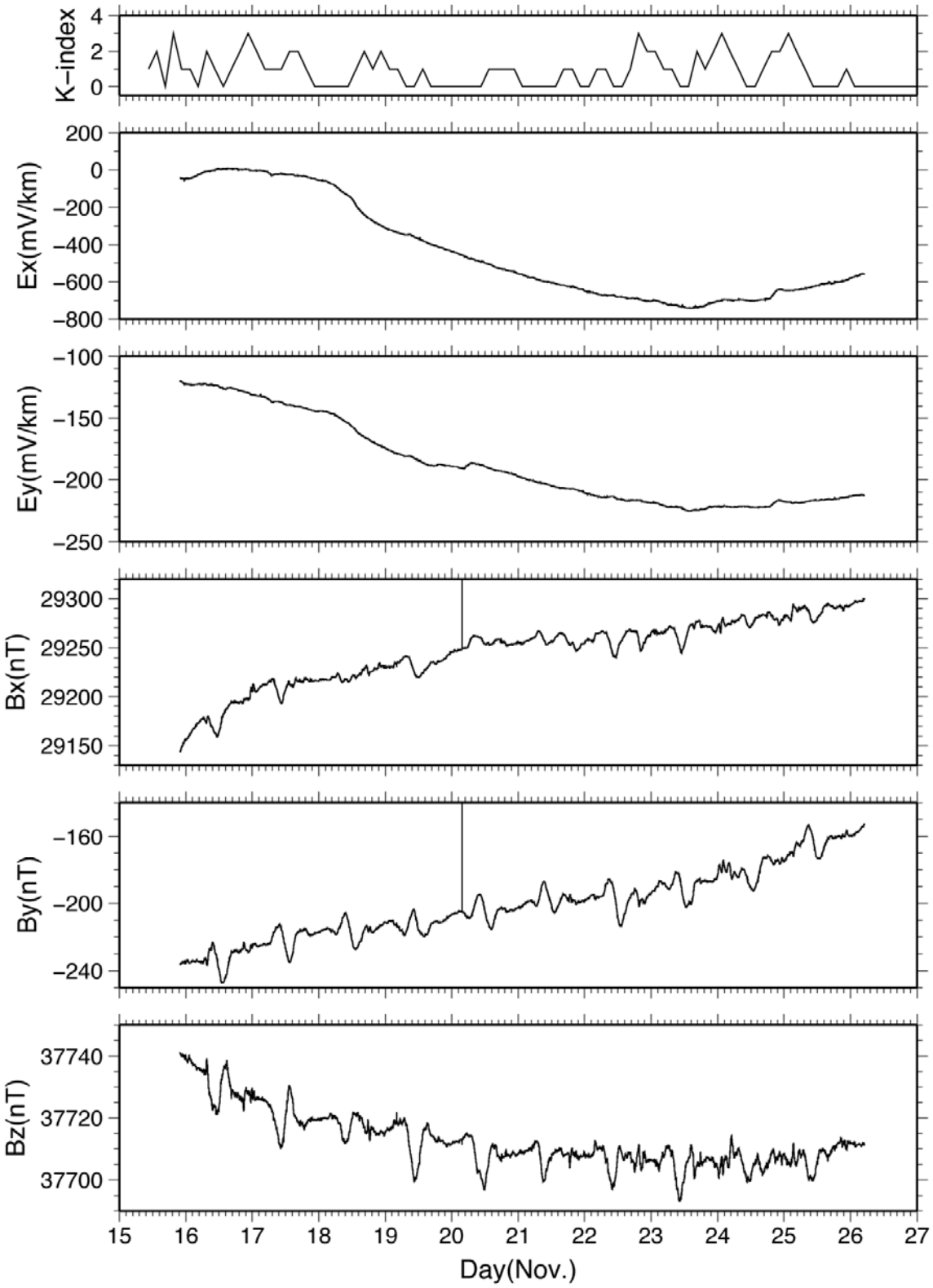

Figure 3.5-9. Corrected time series at site B12 with K-index in Kakioka Magnetic Observatory (in JST).

Table 3.5-5. Azimuth of OBEMs

Site ID	OBEM ID	Azimuth of OBEM (+ clockwise)
C11	JM102	-15.9°
B11	JM103	-63.8°
B12	JM101	-39.5°

3.5.5. Bathymetry and geophysical survey

Bathymetry and geophysical mapping surveys were made mainly at night along the lines listed in the Appendices (7.2). On all the lines, measurements of gravity and three components of the geomagnetic field were conducted with instruments on board as well as bathymetry mapping with a SeaBeam system. The total intensity of the geomagnetic field was measured with a proton precession magnetometer along ENE-WSW lines on the seaward side of the Japan Trench (cf. Fig. 3.2-1). We also made 4 kHz subbottom profiling (SBP Lines 1 to 3) around piston coring sites for imaging structures in surface sediments.

4. Notice on Using

This cruise report is a preliminary documentation as of the end of the cruise.

This report may not be corrected even if changes on contents (i.e. taxonomic classifications) may be found after its publication. This report may also be changed without notice. Data on this cruise report may be raw or unprocessed. If you are going to use or refer to the data written on this report, please ask the Chief Scientist for latest information.

Users of data or results on this cruise report are requested to submit their results to the Data Management Group of JAMSTEC.

5. Acknowledgements

We are grateful to Captain S. Ryono, the officers and the crew of the R/V Kairei for skillful operations of the ship and research equipment. We also extend our thanks to K. Tsukuda, Y. Sato, Y. Matsuura, A. So, and K. Yoshida for giving us great assistance in research works throughout the cruise. The staff of the Operation Group, Research Vessel Management and Operations Department, Marine Technology Center, especially K. Yatsu, made excellent arrangements for the cruise.

The research conducted on this cruise was partly supported by Japan Society for the Promotion of Science and Ministry of Education, Culture, Sports, Science and Technology through Grant-in Aids for Scientific Research (19340125 and 22109510).

6. References

Fujie, G., J. Kasahara, R. Hino, T. Sato, M. Shinohara, and K. Suyehiro, A significant relation between seismic activities and reflection intensities in the Japan Trench region, Geophys. Res. Lett., 29, 7, 10.1029/20, 2002.

Goto, T., H. Mikada, K. Suyehiro, K. Yamane, L. Lewis, A. Orange, E. Nichols, and S. Constable, Electrical conductivity structures across seismically active and less active zones on the subducting Pacific plate, off northeast Japan, Eos Trans. AGU, 82(47), Fall Meet. Suppl.: Abstract GP21A-0249, 2001.

Hamamoto, H., M. Yamano, and S. Goto, S., Heat flow measurement in shallow seas through long-term temperature monitoring, Geophys. Res. Lett., 32, L21311, doi:10.1029/2005GL024138, 2005.

Hirano N, K. Kawamura, M. Hattori, K. Saito, and Y. Ogawa, A new type of intra-plate volcanism; young alkali-basalts discovered from the subducting Pacific Plate, northern Japan Trench, Geophys. Res. Lett., 28, 2719-2722, 2001.

Hirano N, E. Takahashi, J. Yamamoto, N. Abe, S.P. Ingle, I. Kaneoka, T. Hirata, J. Kimura, T. Ishii, Y. Ogawa, S. Machida, and K. Suyehiro, Volcanism in response to plate flexure, Science, 313, 1426-1428, 2006.

Ito, A., G. Fujie, T. Tsuru, S. Kodaira, A. Nakanishi, and Y. Kaneda, Fault plane geometry in the source region of the 1994 Sanriku-oki earthquake, Earth Planet. Sci. Lett., 223, 163-175, 2004

Iwamori, H., Transportation of H_2O beneath the Japan arcs and its implications for global water circulation, Chem. Geol., 239, 182-198, 2007.

Kasaya, T., and T. Goto, A small OBEM and OBE system with an arm folding mechanism, Exploration Geophysics, 40, 41-48, 2009.

Kasaya, T., T. Goto, and R. Takagi, Marine electromagnetic observation technique and its development –For crustal structure survey-, BUTSURI-TANSA, 59, 585-594 (in Japanese with English abstract), 2006.

Miura, S., N. Takahashi, A. Nakanishi, T. Tsuru, S. Kodaira and Y. Kaneda, Structural characteristics off Miyagi forearc region, the Japan Trench seismogenic zone, deduced from a wide-angle reflection and refraction study, Tectonophysics, 407, 165-188, 2005.

Oleskevich, D.A., R.D. Hyndman, and K. Wang,, The updip and downdip limits to great subduction eartquakes: thermal and structural models of Cascadia, south Alaska, SW Japan, and Chile, J. Geophys. Res., 104, 14965-14991, 1999.

Sass, J.H., C. Stone, and R.J. Munroe, Thermal conductivity determinations on solid rocks - a comparison between a steady-state divided-bar apparatus and a commercial transient line-source device, Jour. Volcanol. Geotherm. Res., 20, 145-153, 1984.

Tsuru, T, J.-O. Park, N. Takahashi, S. Kodaira, Y. Kido, Y. Kaneda, and Y. Kono, Tectonic features of the Japan Trench convergent margin off Sanriku, northeastern Japan, revealed by multichannel seismic reflection data, J. Geophys. Res., 105, 16,403-16,413, 2000.

Von Herzen, R., and A.E. Maxwell, The measurement of thermal conductivity of deep-sea sediments by a needle-probe method, J. Geophys. Res., 64, 1557-1563, 1959.

Yamano, M., M. Kinoshita, and S. Goto, High heat flow anomalies on an old oceanic plate observed seaward of the Japan Trench, Int. J. Earth. Sci, 97, 345-352, 2008.

Yamano, M., H. Hamamoto. Y. Kawada, and L. Ray, Heat flow distribution in the northern Japan Trench area and temperature anomaly in the upper part of the Pacific plate, Japan Geoscience Union Meeting 2010, SCG086-10 (abstract), 2010.

Yamanaka, Y., and M. Kikuchi, Asperity map along the subduction zone in northeastern Japan inferred from regional seismic data, J. Geophys. Res., 109, B07307, doi:10.1029/2003JB002683, 2004.

7. Appendices

7.1. Cruise Log

Date	Time	Description	Ship position / Weather Sea condition (Noon@JST)
14-Nov	08:00	Scientist party on board a ship	34-50.5N,139-54.0E
	09:00	Departure from JAMSTEC (The KR10-12 cruise started)	Overcast
	10:00-11:00	Briefing about ship's life and safety	Wind:NW-Gentle breeze
	14:00	Arrived at research area "H"	Wave:2 (Calm)
	14:40	Release command of pop-up water temperature monitoring system	Swell:2 (Low Swell long)
	15:25	Recovery of pop-up water temperature monitoring system	
	15:45-16:30	Figure eight turn (Magnetic calibration)	
	16:30	Transit to area "F"(Site C11)	
	18:00-18:30	Scientist meeting	
15-Nov	07:00	Arrived at research area "F"(Site C11)	39-05.0N,142-26.8E
	08:27	Deployment of pop-up OBEM (Site C11)	Cloudy
	12:27	Release of XBT at 39-11.0878N, 142-28.0264E	Wind:NW-Moderate breeze
	12:56-13:32	The MBES survey (OBEM Site preliminary survey)	Wave:3 (Slight)
	14:22	Deployment of pop-up OBEM (Site B11)	Swell:2 (Low Swell long)
	16:16	Deployment of pop-up OBEM (Site B12)	
	18:00-18:30	Scientist meeting	
	18:11-23:14	The MBES survey (Line 1)	
16-Nov	06:00	Release of XBT at 39-07.1215N, 143-57.6319E	39-04.8N,144-49.0E
	06:27	Deployment of pop-up OBEM (Site B13)	Overcast
	12:22	Deployment of pop-up OBEM (Site B14)	Wind:NW-Strong breeze
	15:14-15:52	The SBP survey (SBP Line 1)	Wave:4 (Moderate)
	15:56	Deployment of proton magnetometer	Swell:4 (Moderate average)
	16:16	The MBES survey commenced (Line 2,3)	
	18:00-18:30	Scientist meeting	
17-Nov	01:50	The MBES survey finished (Line 2,3)	39-02.0N,144-48.5E
	05:58	Recovery of proton magnetometer	Fine but cloudy
	10:00-14:13	Piston core sampling with heat flow measurement (HFPC01)	Wind:Calm
	15:53-20:33	Heat flow measurement (HF01)	Wave:1 (Calm)
	20:45	Transit to MIYAKO	Swell:1 (Low swell short)
18-Nov	07:50	Arrived at Off-MIYAKO port	39-37.9N,141-59.2E
	08:43-09:39	Disembarkation of scientists (2 persons)	Fine but cloudy
	09:30-10:00	Scientist meeting	Wind:ENE-Light breeze
	16:30-17:00	Pick-up of tranceponder	Wave:1 (Calm)
	17:45	Transit to area"A" (HF02)	Swell:1 (Low swell short)
	18:00-18:30	Scientist meeting	
19-Nov	06:20	Arrived at research area "A"(HF02)	40-14.5N,145-40.5E
	06:20	Release of XBT at 40-13.9260N, 145-41.4118E	Fine but cloudy
	07:55-18:13	Heat flow measurement (HF02)	Wind:ENE-Gentle breeze
	18:30	Deployment of proton magnetometer	Wave:2 (Smooth)
	18:40-19:30	Figure eight turn (Magnetic calibration)	Swell:3 (Moderate short)
	19:00-19:15	Scientist meeting	
	23:45	The MBES survey commenced (Line 4)	

Date	Time	Description	Ship position / Weather Sea condition (Noon@JST)
20-Nov	02:30	The MBES survey finished (Line 4)	38-46.5N,146-43.0E
	04:58	Arrived at research area "B"(HFPC02)	Fine but cloudy
	04:58	Release of XBT at 38-51.0061N, 147-03.9501E	Wind:East-Gentle breeze
	05:18-05:45	The MBES survey (Line 5)	Wave:2 (Smooth)
	06:01	Recovery of proton magnetometer	Swell:2 (Low swell long)
	06:43-10:44	Piston core sampling with heat flow measurement (HFPC02)	
	12:35-17:54	Heat flow measurement (HF03)	
	18:09	Deployment of proton magnetometer	
	19:00-19:15	Scientist meeting	
	20:45	The MBES survey commenced (Line 6)	
21-Nov	04:40	The MBES survey finished (Line 6)	39-59.8N,145-05.7E
	05:55	Recovery of proton magnetometer	Fine but cloudy
	06:30-11:54	Heat flow measurement (HF04)	Wind:East-Gentle breeze
	14:12-19:09	Heat flow measurement (HF05)	Wave:2 (Smooth)
	19:23	Deployment of proton magnetometer	Swell:2 (Low swell long)
	19:30-19:45	Scientist meeting	
	21:16-23:41	The MBES survey (Line 7)	
22-Nov	06:08	Recovery of proton magnetometer	40-15.0N,146-46.0E
	06:12	Release of XBT at 40-13.8618N, 146-53.3033E	Blue sky
	06:38-11:08	Heat flow measurement (HF06)	Wind:SSE-Fresh breeze
	12:33-17:02	Heat flow measurement (HF07)	Wave:3 (Slight)
	17:17	Deployment of proton magnetometer	Swell:3 (Moderate short)
	17:39-18:21	Figure eight turn (Magnetic calibration)	
	18:30-18:45	Scientist meeting	
	20:21	The MBES survey commenced.	
23-Nov	04:57	The MBES survey finished	38-30.0N,142-26.5E
	06:36	Recovery of proton magnetometer	Rain
	06:37	Transit to ISHINOMAKI	Wind:North-Near gale
	16:44	Arrived at Off-ISHINOMAKI port	Wave:6 (Very rough)
			Swell:5 (Moderate long)
24-Nov	09:00-10:00	Onboard excursion	38-22.3N,141-19.0E
	10:00-11:00	Onboard seminar	Fine but cloudy
	16:00	Transit to area "F"(C11)	Wind:NW-Light air
			Wave:1 (Calm)
			Swell:0 (No swell)
25-Nov	06:00	Arrived at research area "F"(Site C11)	38-19.6N,142-26.4E
		It has not recovered though it stood by until the sea condition recovers.	Fine but cloudy
	14:35	Transit to Site B11	Wind:SE-Light breeze
		It has not recovered though it stood by until the sea condition recovers.	Wave:1 (Calm)
	19:00	Arrived at Site B11	Swell:5 (Moderate long)
26-Nov	04:00	Transit to Site B12	38-22.0N,142-20.0E
	05:45	Arrived at Site B12	Overcast
	05:47	Release command of pop-up OBEM (Site B12)	Wind:North-Light breeze
	06:42	Recovery of pop-up OBEM (Site B12)	Wave:2 (Smooth)
	07:57	Release command of pop-up OBEM (Site B11)	Swell:2 (Low swell long)
	08:39	Recovery of pop-up OBEM (Site B11)	
	12:36	Release command of pop-up OBEM (Site C11)	
	13:19	Recovery of pop-up OBEM (Site C11)	
	13:28	Deployment of proton magnetometer	
	13:48-14:29	Figure eight turn (Magnetic calibration)	
	18:30-18:45	Scientist meeting	
	22:09	The MBES survey commenced (Line 9)	

Date	Time	Description	Ship position / Weather Sea condition (Noon@JST)
27-Nov	02:00	The MBES survey finished (Line 9)	39-10.0N,143-39.0E
	07:45	Arrived at	Fine but cloudy
	07:44-08:38	The SBP survey (SBP Line 2,3)	Wind:NW-Fresh breeze
	08:47	Recovery of proton magnetometer	Wave:5 (Moderate)
	13:20-16:29	Piston core sampling with heat flow measurement (HFPC03)	Swell:3 (Moderate short)
	17:00	Transit to JAMSTEC	
28-Nov	09:00-09:15	Scientist meeting	35-25.0N,140-50.5E
	20:30	Arrived at TOKYO-Bay Area 4	Fine but cloudy
			Wind:SW-Gale
			Wave:6 (Very rough)
			Swell:4 (Moderate average)
29-Nov	09:00	Arrived at JAMSTEC	
		The KR10-12 cruise end and the scientist party left the ship	

SWELL SCALE

0:No swell
1:Low swell short
2:Low swell long
3:Moderate short
4:Moderate average — Weak wave (Under 2m)
5:Moderate long
6:Heavy swell short
7:Heavy swell average
8:Heavy swell long — Big wave a little (2 - 4m)
9:Confused swell — Big wave (Over 4m)

WIND SCALE

0:Calm	0 - 0.2m/sec
1:Light air	0.3 - 1.5m/sec
2:Light breeze	1.6 - 3.3m/sec
3:Gentle breeze	3.4 - 5.4m/sec
4:Moderate breeze	5.5 - 7.9m/sec
5:Fresh breeze	8.0 - 10.7m/sec
6:Strong breeze	10.8 - 13.8m/sec
7:Near gale	13.9 - 17.1m/sec
8:Gale	17.2 - 20.7m/sec
9:Strong gale	20.8 - 24.4m/sec
10:Storm	24.5 - 28.4m/sec
11:Violent storm	28.5 - 32.6m/sec
12:Hurricane	Over 32.7m/sec

short : wavelength under 100m (Cycle : Under 8.0sec)
average : wavelength 100 - 200m (Cycle : 8.1 - 11.3sec)
long : wavelength under 200m (Cycle : Over 11.4sec)

7.2. Bathymetry and Geophysical Survey

[Bathymetry survey lines]

Line Name	Start				End				Remarks
	Date	Time (UTC)	Latitude	Longitude	Date	Time (UTC)	Latitude	Longitude	
Line 1	11.15	09:11	39-14.6329N	142-24.7842E	11.15	14:14	38-14.9896N	142-17.3829E	
Line 2	11.16	07:16	38-54.6003N	144-49.0408E	11.16	09:18	38-45.9384N	144-19.7954E	(*1)
Line 3	11.16	09:57	38-38.9772N	144-19.9108E	11.16	16:50	39-08.8015N	146-00.4014E	(*1)
Line 4	11.19	14:45	39-08.6665N	145-59.9078E	11.19	17:30	39-20.8064N	146-40.7224E	(*1)
Line 5	11.19	20:18	38-48.1293N	147-03.9835E	11.19	20:45	38-42.3616N	147-04.0033E	(*1)
Line 6	11.20	11:45	39-21.3491N	147-05.9164E	11.20	19:40	38-46.6242N	145-09.1027E	(*1)
Line 7	11.21	12:16	38-54.5074N	144-48.7113E	11.21	14:41	39-04.9764N	145-23.8230E	(*1)
Line 8	11.22	11:21	39-47.9198N	146-40.1388E	11.22	19:57	39-04.8019N	144-34.4441E	(*1)
Line 9	11.26	13:09	38-57.9555N	144-34.8661E	11.26	17:00	39-19.7074N	145-27.5995E	(*1)
SPB Line 1	11.16	06:16	39-01.9776N	144-48.9739E	11.16	06:52	38-55.9477N	144-48.9834E	
SPB Line 2	11.26	22:44	39-06.7901N	143-39.9853E	11.26	23:05	39-09.6172N	143-40.0006E	
SPB Line 3	11.26	23:22	39-08.5416N	143-41.0944E	11.26	23:38	39-08.5398N	143-38.7951E	

(*1) The Proton magnetometer was towed.

(*2) Equipment information

Multi-narrow Beam Echo Sounder

Manufacturer : SeaBeam Instruments

Type : Sea Beam 2112.004

[Gravity measurement]

Date	Time (UTC)	Comment	Remarks
11.14	00:00		Departure:Private quay for JAMSTEC
11.14	00:12	Sea State 2 → 4	
11.28	23:40		Arrival:Private quay for JAMSTEC
11.29	00:03	Sea State 4 → 2	

(*1) Data is always being collected.

(*2) Equipment information

Shipboard gravimeter

Manufacturer : Fuguro Co., Ltd.

Type : BODESEEWERK KSS31

[Geomagnetic field measurement]

Date	Time (UTC)	Comment	Remarks
11.14	00:10	Three-component magnetometer record started	Departure:Private quay for JAMSTEC
	06:45	"Figure of 8" started	34-30.0N 140-30.0E
	07:30	"Figure of 8" finished	
11.16	07:07	Proton magnetometer record started	
	20:49	Proton magnetometer record finished	
11.18	09:40	"Figure of 8" started	40-13.0N 145-42.5E
	10:30	"Figure of 8" finished	
11.19	09:34	Proton magnetometer record started	
	20:54	Proton magnetometer record finished	
11.20	09:15	Proton magnetometer record started	
	20:49	Proton magnetometer record finished	
11.21	10:27	Proton magnetometer record started	
	20:57	Proton magnetometer record finished	
11.22	08:22	Proton magnetometer record started	
11.22	08:39	"Figure of 8" started	40-12.0N 146-40.0E
	09:21	"Figure of 8" finished	
	21:27	Proton magnetometer record finished	
11.26	02:36	Proton magnetometer record started	
	23:41	Proton magnetometer record finished	
11.26	04:48	"Figure of 8" started	38-18.0N 142-24.0E
	05:29	"Figure of 8" finished	
11.28	23:56	Three-component magnetometer record finished	Arrival:Private quay for JAMSTEC

(*1) Equipment information

Three-component magnetometer

Manufacturer : Tiera technica

Type : SFG1214

Proton magnetometer

Manufacturer : Kawasaki Geological Engineering Co. Ltd.

Type : PROTO10